DESORPTION KINETICS OF TRACE ORGANIC CONTAMINANTS AND NATURAL ORGANIC MATTER FROM SUPERFINE POWDERED ACTIVATED CARBON

A Thesis
Presented to
the Graduate School of
Clemson University

In Partial Fulfillment
of the Requirements for the Degree
Master of Science
Environmental Engineering and Earth Science

---

by
Misty Brown
August 2016

Accepted by:
Dr. David Ladner, Committee Chair
Dr. Tanju Karanfil
Dr. Ezra Cates

ABSTRACT

Powdered activated carbon (PAC) particles that have been ground to a submicron size are being studied for use as an adsorbent during the water treatment process. These superfine powdered activated carbon (S-PAC) particles can be used for the removal of trace contaminants and natural organic matter (NOM) from water. It has been shown that these smaller particles have faster adsorption kinetics and an increased adsorption capacity for NOM due to their larger specific surface area and shorter internal diffusion rate into the particles.

One thing that has not been studied is the desorption kinetics of trace contaminants on these S-PAC particles. Desorption is typically not an issue in real systems as long as the effluent concentration remains below regulatory limits; however, it could become a problem when the carbon residence time in an absorber is greater than the hydraulic residence time. If there are high transient loadings of strongly competing compounds, these compounds can displace the more weakly adsorbing contaminants. This would result in a shorter adsorbent life.

The main objectives behind studying the desorption kinetics of trace contaminants on S-PAC were to improve our understanding of the characteristics of S-PAC by: (i) measuring the desorption kinetics of trace contaminants on S-PAC when in competition with a strongly competing compound and (ii) measuring the desorption kinetics of trace contaminants on S-PAC when in competition with a strongly competing compound and a pore blocking organic compound. A bituminous coal based activated carbon, WC800, and a wood based activated carbon, Aqua Nuchar, were used as the adsorbent materials in this study. Radiolabeled atrazine was used as the model trace contaminant, 1,4-dichlorobenzene (p-DCB) was used as the model

strongly competing compound, and Suwanee River natural organic matter (SRNOM) was used as the model pore blocking organic matter.

The desorption kinetics of atrazine were faster for S-PAC than PAC for WC800 and Aqua Nuchar activated carbon. This is because of the larger fraction of external surface area and shorter internal diffusion length on the smaller particles. However, after the 30 minute milling time, there appears to be no trend in desorption kinetics. A two-step time dependence showing a fast initial desorption of atrazine followed by a slower, diffusion limited step of internally absorbed material can be seen for the S-PAC milling times.

It was also found that NOM does not block as many pores on the S-PAC due to the larger specific external surface area. This allowed p-DCB to displace the atrazine faster on the WC800 and Aqua Nuchar S-PAC particles. Desorption kinetics are faster without SRNOM in the water because there is less competition from pore blockage. There is also less SRNOM competition on the S-PAC particles than there is on the PAC, therefore the desorption kinetics on S-PAC are faster than on PAC when SRNOM is present.

DEDICATION

I would like to dedicate this thesis to my parents, Rob and Kim Brown, and my grandparents, Dorlan and Janie Vanderpool, for all of their encouragement and support.

ACKNOWLEDGEMENTS

I would like to thank my advisor, Dr. Ladner, who gave me the opportunity to work on this project and for his constant guidance throughout my graduate school career. I would also like to acknowledge Dr. Karanfil and Dr. Cates for their willingness to be a part of my committee, for their useful comments on my proposal and thesis and for their help throughout this process.

I would like to acknowledge Dr. Priscilla To for her dissertation work on the desorption kinetics of trace contaminants and pore blocking organic matter from PAC and for her help developing my experimental setup. Along with her experimental setup and research plan, her HSDM model was very useful in helping me model my own data. I would also like to acknowledge Katie Davis for providing me with the SEM images that were used to show the activated carbon on membranes in my thesis.

Finally, I want to say thank you to my lab group for helping me learn to use all of the equipment in the lab and for the useful comments during our weekly group meetings that helped me improve my thesis work. I also want to thank all of my friends and family for supporting me and encouraging me for the past two years that I have been at Clemson University.

Materials and supplies for this project were provided through a grant from the National Science Foundation, CBET 1236070.

TABLE OF CONTENTS

Page

Table of Contents (continued)

Page

Table of Contents (continued)

Page

LIST OF TABLES

Table Page

LIST OF FIGURES

Figure Page

List of Figures (continued)

Figure Page

List of Figures (continued)

Figure Page

LIST OF ABBREVIATIONS AND SYMBOLS

Abbreviations

BET	Brunauer-Emmett-Teller
EBC	Equivalent Background Compound
DBP	Disinfection Byproduct
DDI	Distilled Deionized Water
DLS	Dynamic Light Scattering
DOC	Dissolved Organic Carbon
GAC	Granular Activated Carbon
HSDM	Homogeneous Surface Diffusion Model
IUAPC	International Union of Pure and Applied Chemistry
LSC	Liquid Scintillation Counting
MIB	2-Methylisoborneol
NOM	Natural Organic Matter
p-DCB	1,4-Dichlorobenzene
PAC	Powdered Activated Carbon
pH	$-\log[H^+]$
pH_{IEP}	Isoelectric Point
pH_{PZC}	Point of Zero Charge
PSD	Pore Size Distribution
PSS	Polystyrene Sulfonate
PVDF	Polyvinylidene Difluoride
SEM	Scanning Electron Microscope
SOC	Synthetic Organic Chemical

SRNOM	Suwanee River Natural Organic Matter
S-PAC	Superfine Particle Activated Carbon
TCE	Trichloroethylene
USEPA	United States Environmental Protection Agency
WC800	Watercarb 800

Symbols

C_c	Carbon concentration
C_o	Initial liquid phase concentration of the trace contaminant
D_s	Diffusivity coefficient
d_t	Incremental time step
K_f	Freundlich equilibrium K parameter for trace compound
1/n	Freundlich equilibrium 1/n parameter for trace compound
n_r	Number of radial increments
q_o	Initial solid phase concentration of the trace contaminant
R	Particle radius
t_f	End time

1 INTRODUCTION

Powdered activated carbon (PAC) is commonly used to remove trace-contaminant synthetic organic chemicals (SOCs) from drinking water. SOCs such as pesticides and personal care products, found in drinking water supplies are potentially hazardous to public health. The large surface area and high-number of adsorption sites on PAC make it ideal for adsorbing these contaminants (Bansal et al., 2010) and its use has made a significant impact on improving the quality of drinking water.

Recently, superfine powdered activated carbon (S-PAC) has been studied as an alternative to PAC. S-PAC is made from a parent PAC material that is ground to a submicron range using a wet milling process (MiniCer, Netzch Premier Technologies, Exton, PA, USA). Typical PAC materials range in particle size from 10 to 50 µm while typical S-PAC particles range in size from 0.1 to 1 µm (Partlan et al., 2016). When the PAC particles are milled into superfine particles, the external surface area of the carbon is increased and a larger fraction of the internal pore volume becomes accessible. These smaller particles of carbon also have a shorter internal diffusion distance to the adsorption sites on the carbon (Matsui et al., 2011).

Due to the larger volume of external surface area and the shorter internal diffusion distance on these smaller particles of carbon, S-PAC has been shown to have faster adsorption kinetics than PAC (Pelekani et al., 2000). Many studies have also shown an improved adsorbate uptake capacity when using S-PAC versus PAC with compounds such as polystyrene sulfonate (PSS) and natural organic matter (NOM) and an improved adsorbate uptake rate with compounds such as geosmin and atrazine (Ando et al., 2010; Ellerie et al., 2013; Matsui, Ando, et al., 2009).

There have been several thorough studies on the adsorption kinetics of S-PAC, however research on the desorption kinetics of these small particles is insufficient. Since adsorption occurs differently on S-PAC as compared to PAC, it is expected that desorption will also occur differently. It is hypothesized that the desorption kinetics of S-PAC will be faster than the desorption kinetics of PAC due to the increased specific external surface area. It is also hypothesized that NOM, which primarily adsorbs on the external surfaces of the carbon and cannot diffuse into the smaller pores, will cause pore blockage on a smaller fraction of S-PAC external surface area than PAC, thus leading to a higher desorption rate of trace contaminants on S-PAC particles. The main motivation for studying these desorption kinetics of S-PAC is to improve the understanding of S-PAC characteristics and to further develop the understanding of the desorption kinetics of trace contaminants from both PAC and S-PAC.

2 BACKGROUND

2.1 Activated Carbon

According to the definition given by the International Union of Pure and Applied Chemistry (IUPAC), activated carbon is defined as "a porous carbon material, a char which has been subjected to reaction with gases, sometimes with the addition of chemicals, e.g. $ZnCl_2$, before, during or after carbonization in order to increase its adsorptive properties" (Fitzer et al., 1995). Activated carbon is widely used for treating water and the main motivation behind this is because of its high adsorption capacity for organic contaminants due to the porous structure created during the activation process. According to the United States Environmental Protection Agency (USEPA), activated carbon adsorption is a best available technology to remove SOCs from drinking water (USEPA, 1986). It can be applied either as PAC, with typical particle sizes ranging from 10 to 50 μm, or as granular activated carbon (GAC), with typical particle sizes ranging between 200 and 1000 μm (Snoeyink et al., 1985).

2.1.1 Origin and Production of Activated Carbon

Most commercially available activated carbons that are used in water treatment come from naturally occurring materials such as coal, wood, peat, and coconut shell. These materials have a high carbon content, low inorganic content, and are relatively economical (Wu et al., 2001). The internal pore structure, surface area distribution, and surface chemistry of the carbon are all a result of the choice of raw material selected to make the activated carbon as well as the activation technique (Bansal et al., 2010).

Activated carbon is generally produced using either a chemical or thermal activation method. The properties of the activated carbon can vary depending on the activation method that is used, which in turn influences the adsorption capabilities of the carbon particles (Okada et al., 2003). Porous materials can be "activated" by carbonizing the raw materials, or extracting the pure carbon from the material by adding heat, and then introducing an oxidizing agent, such as steam or carbon dioxide during the thermal activation process or an acid-base chemical treatment during the chemical activation process (Li et al., 2003a; Summers et al., 2010; Wigmans, 1989). These activation processes create a continuous pore structure within the carbon that results in an increase in internal surface area and micropore volume and also makes it ideal for trace contaminant adsorption.

2.1.2 Structures of Activated Carbon

Activated carbon has a microcrystalline structure that is composed of carbon atoms ordered in parallel stacks of hexagonal layers (Karanfil et al., 1999). This structure forms a carbon with various pore sizes and shapes. There are three different types of pore sizes: macropores, mesopores, and micropores. According to the IUPAC convention, a macropore is greater than 500 angstroms in size, a mesopore is between 20 and 500 angstroms, secondary micropores range from 8 to 20 angstroms and primary micropores are less than 8 angstroms (Sing et al., 1985). **Figure 2.1** shows examples of mesopores, micropores, and macropores on a GAC particle.

The pore size distribution of activated carbon is significant because along with surface area and pore volume, it is one of the most important factors when determining the adsorption capacity of an activated carbon. Li et al. (2003b) found that PACs with larger pore size distributions were affected less by pore blockage from NOM than PACs with a smaller fraction of

large pores. Pelekani et al. (2000) found that adsorption equilibrium for atrazine and methylene blue was achieved more rapidly with increasing average pore size and total pore volume for five different activated carbon fibers.

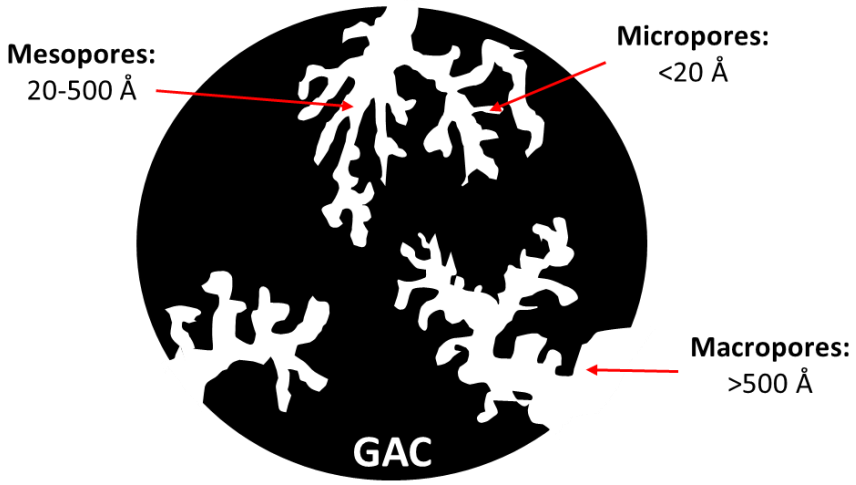

Figure 2.1 Schematic pore structure of GAC (Hopman et al., 1995).

2.1.3 Applications of Activated Carbon

Activated carbon is used for many things, such as drinking water treatment, medical applications, and industrial processes. However, drinking water treatment is the main use of activated carbon in the United States. Drinking water treatment employs the process of adsorption to remove organic contaminants such as taste, odor, and color producing compounds and SOCs from water (Lemley et al., 1995). During the adsorption process, adsorbates accumulate on the surfaces of the carbon until the adsorption capacity is reached (Sontheimer et al., 1988). The large surface area of the activated carbon binds adsorbates using Van der Waals forces, where electrons are shared between the carbon and the contaminants

and a bond is created between the two. This large surface area and the high affinity for a broad range of organic compounds is what makes activated carbon so good for adsorption processes.

2.2 Superfine Powdered Activated Carbon

S-PAC is created from a parent PAC material that is ground to a submicron range and usually varies in size from 0.1 to 1 microns. The use of S-PAC has shown improved kinetics for removing trace contaminants and SOCs from water over PAC. The faster adsorption kinetics can be attributed to the larger external specific surface area per unit mass and also the shorter internal diffusion rate into the particles (Adham et al., 1991; Ando et al., 2010; Dunn et al., 2013; Matsui et al., 2008, 2015).

Matsui et al. also found that S-PAC can remove the same amount of trace contaminants in the same contact time using a lower activated carbon dosage than required for PAC. The dosage savings from using S-PAC instead of PAC was found to be at least 75% (Matsui et al., 2007). After 30 minutes of contact time using the same PAC and S-PAC dosage, 90% of geosmin was removed from water using S-PAC while only 30% of the geosmin was removed from the water using PAC (Matsui et al., 2009).When using S-PAC to treat effluent wastewater, it was found that S-PAC application resulted in up to two times more dissolved organic carbon (DOC) removal in comparison to PAC. This translates to a reduced contact time, carbon dosage and tank size requirements while using the same activated carbon loading for S-PAC and PAC (Bonvin et al., 2015). In addition to providing improved kinetics and lower dosage requirements, these small particles have also been found to perform better in the presence of NOM, establishing them as superior to PAC (Heijman et al., 2009; Matsui et al., 2013; Matsui et al., 2009). NOM adsorption

occurs mainly at the external region of the carbon particles with little diffusion into the adsorbent, so the increased specific external surface area of S-PAC also increases the adsorption capacity for NOM (Ando et al., 2010; Matsui et al., 2011).

2.2.1 Surface Area and Particle Size of S-PAC

Particle size and surface area are parameters that have been shown to be an important indicator for activated carbon adsorption capacity. Partlan et al. (2016) found that as the milling time of a carbon particle is increased, the mean particle size of the activated carbon is decreased. Studies by Ando et al. (2010) found that S-PAC had a much higher adsorption capacity than PAC over five different carbons. The larger specific external surface area per of the smaller particles translate into a higher adsorption capacity for large molecular weight molecules, such as NOM. **Figure 2.2** shows the wet milling process of creating S-PAC particles from a parent PAC material and how the specific external surface area is increased with

increased milling time. The oxygen content of the S-PAC also increases with increasing specific external surface area, which can be seen in **Figure *2.2*** as well.

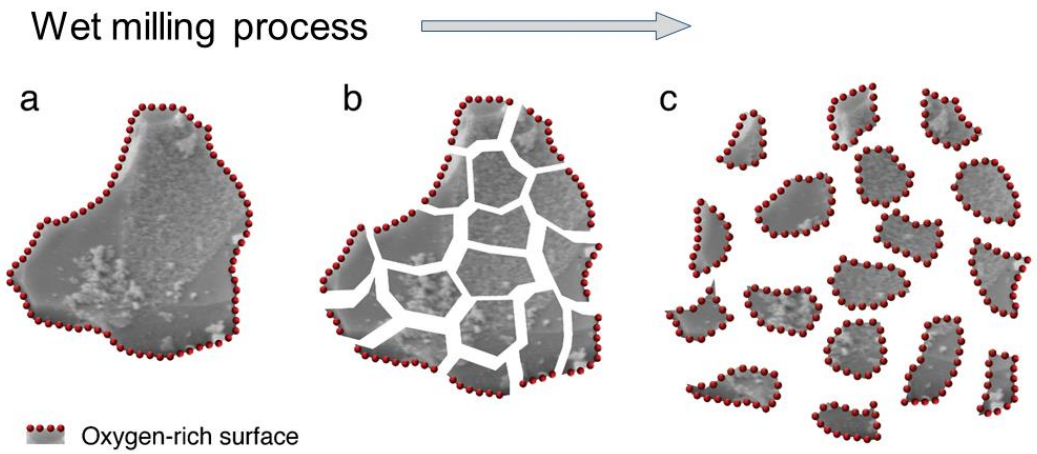

Figure 2.2 Wet milling process (Partlan et al., 2016).

2.2.2 Pore Size Distribution of S-PAC

The percentage of total pore volume that falls into the categories of macropores, mesopores and micropores also plays an important role in the adsorption capacity for NOM and trace contaminants on activated carbon. A macropore is considered anything that is greater than 50 nm, a mesopore is between 2 nm and 50 nm, and a micropore is smaller than 2 nm (Partlan et al., 2016). The total pore size distribution of these three type of pores on an activated carbon particle governs the fraction of pore volume that can be accessed by an adsorbate of a specific size (Pelekani et al., 1999). The higher energy adsorption sites on a particle of activated carbon correspond to the smaller pores because of overlapping adsorption potentials (Li et al., 2002).

In one study investigating the importance of pore size distribution for competitive adsorption, Pelekani and Snoeyink used atrazine and Congo red dye on five activated carbon

fibers with different pore sizes. It was found that the atrazine adsorption capacity was higher than the Congo red adsorption capacity for all carbon fibers tested because of its smaller size and ability to access the smaller micropores. Congo red caused pore blockage on the activated carbon fibers, but it did not displace the atrazine because the two compounds were not competing for the same adsorption sites. However, because of the pore blockage caused by the Congo red, the atrazine adsorption capacity of the activated carbon fibers was greatly reduced (Pelekani et al., 2001).

Other studies using trichloroethylene (TCE) and other SOCs in competition with NOM have had similar findings. In one example, Li et al. (2003a) found that high molecular weight NOM can cause pore blockage on carbons that have a high percentage of micropores, but this pore blockage effect was greatly alleviated on highly mesoporous carbons. According to a study by Kilduff and Karanfil (1998), low molecular weight compounds have the greatest effect on the reduced adsorption capacity of TCE on GAC because the high molecular weight NOM compounds cannot compete for the same sites on the activated carbon as TCE. Low molecular weight compounds that are preloaded on GAC preferentially occupy the high-energy adsorption sites, which makes these sites unavailable for SOC adsorption.

It has also been determined by Ebie et al. (2001)and Li et al. (2003a) that a carbon with a higher percentage of mesopores is less affected by pore blockage from NOM during adsorption and therefore, a carbon with a larger pore size distribution is ideal to use for treating water that contains NOM. Increasing the pore size distribution of microporous carbons could alleviate the pore blockage affect caused by NOM and also increase the trace contaminant adsorption capacity (Pelekani et al., 1999).

It is a well-known fact that the pore size distribution of activated carbon plays an important role in its adsorption capacity. Some studies have found that when PAC particles are milled into smaller S-PAC particles, there could be a shift in the distribution of the pore sizes as smaller diameter pores are exposed to create larger diameter pores (Dunn et al., 2013; Ellerie et al., 2013; Matsui et al., 2014). Some studies found that S-PAC particles had lower micropore and higher mesopore volumes than PAC, which increased the adsorption of trace compounds, such as methylene blue (Ellerie et al., 2013; Matsui et al., 2004). Partlan et al. (2016) observed little change in the micropore fraction with increased milling time for coal, wood and coconut shell based carbons. However, the coal based carbons showed an increase in the mesoporous fraction as a result of increased milling, while the wood based carbon showed a decreased mesoporous fraction.

2.2.3 Surface Chemistry of S-PAC

Functional groups on the particle surface influence the adsorption properties of activated carbon. Contaminants exhibit various affinities for different surface functional groups depending on the molecule structure. The acidity and basicity of an activated carbon surface are determined by oxygen and nitrogen containing surface functional groups, respectively (Mangun et al., 2001). Increasing the oxygen containing functional groups on the surface of an activated carbon increases the acidity of the carbon, which decreases the adsorption affinity of organic molecules (Coughlin et al., 1968; Garcia et al., 2004; Karanfil et al., 1999; Li et al., 2002). The surface acidity of an activated carbon also elicits water adsorption on the carbon, which decreases the contaminant uptake capacity. These water molecules can adsorb on hydrophilic oxygen groups using hydrogen bonding to form water clusters that block the adsorption sites

(Franz et al., 2000; Kose, 2010; Quinlivan et al., 2005). Kilduff and Karanfil (2002) showed that the more hydrophobic carbon with less surface acidity had the largest adsorption capacity for TCE with and without preloaded NOM. Garcia et al. (2004) showed that higher concentrations of surface oxygen groups on an activated carbon resulted in lower adsorption capacity than activated carbons with a lower percent of surface oxygen groups.

There have only been a few studies that have looked at the surface chemistry on different mean sizes of S-PAC. Partlan et al. (2016) found that the oxygen content increased and the point of zero charge (pH_{PZC}) decreased with milling time for all adsorbents that were tested. The pH_{PZC} describes the condition in which the electrical charge density on the surface of the carbon is zero and the values indicate the acidity/basicity characteristics of an activated carbon and can alter preferential adsorption with respect to the adsorbate charge (Dastgheib et al., 2004). The increase in oxygen content can results in a decrease in the adsorption of organic compounds (Considine et al., 2001; Karanfil et al., 1999). The isoelectric point (pH_{IEP}), which is the pH when a particle of carbon has no net electrical charge, did not change significantly with milling and did not correlate with the oxygen increase, which is thought to be because oxidation occurs primarily and readily on the external surfaces (Partlan et al., 2016).

2.2.4 Challenges with Using S-PAC

One challenge that has been found with using S-PAC for contaminant removal from water is that it cannot be removed as easily from the treated water as PAC. Generally, PAC is removed from water treatment systems using coagulation/flocculation and sedimentation. There are currently studies being done on the coagulation/flocculation and sedimentation on S-PAC, but for now since S-PAC cannot be settled out in any reasonable time, it has the ability to pass into

the treated drinking water. Coupling S-PAC with membranes could be one way to mitigate this problem. The membranes will stop the S-PAC from passing into the treated water while the S-PAC still attains the improved adsorption kinetics. The issue with coupling these small particles with membranes is that small particles will cause more membrane fouling than other larger adsorbents due to cake formation on the membrane and pore clogging of the membrane. This will decrease the flux of water through the membrane and result in higher energy requirements and a higher cost of treating water (Ellerie et al., 2013).

2.3 Natural Organic Matter

Dissolved NOM, found in most drinking water sources, is a mixture of humic and non-humic organic molecules with a range of molecular weights (Chi et al., 2004). Some of the smaller NOM molecules can compete for the same sites on activated carbon as many trace contaminants while the larger NOM molecules can cause pore blockage on the activated carbon particles. One of the main reasons that NOM competition is so important is because in natural waters the NOM concentration is usually several orders of magnitude greater than the concentration of micorpollutants. It is also important to remove NOM before the disinfection process because NOM is a precursor to disinfection byproducts (DBPs) which form from a reaction with chemical, organic and inorganic substances and are potentially harmful to human health (Karanfil et al., 1999).

The different organic molecules found in dissolved NOM can also have a negative impact on the adsorption capacity of activated carbon and the kinetics of trace contaminant adsorption. NOM preferentially adsorbs near the outer surface of carbon particles with little on the inside

regions (Ando et al., 2011; Matsui et al., 2014). These NOM particles can block the pores on the activated carbon making the internal adsorption sites inaccessible and decreasing the adsorption capacity of trace contaminants (Li et al., 2002).

2.3.1 NOM Effect on S-PAC Adsorption

NOM has been shown to have a negative impact on the adsorption of trace contaminants onto activated carbon. One advantage that has been found with using S-PAC instead of PAC is that the negative effects on trace contaminant adsorption caused by NOM are reduced. Since there is more external surface area on S-PAC in comparison to PAC, S-PAC has a higher adsorption capacity for NOM. S-PAC has a greater ratio of external adsorption capacity to internal adsorption capacity when compared to PAC, so competition between NOM and SOCs is reduced, even when some of the pores are being blocked by the NOM (Matsui et al., 2012). However, on the smaller particles of activated carbon, there is less distance between internal and external adsorption sites. It is suspected that even if NOM blocks the pores in these small particles, it is more likely to desorb and allow for trace-contaminant adsorption because the pore blockage is not as deep.

Newcombe et al. (2002) found that low molecular weight NOM molecules competed directly with 2-methylisoborneol (MIB) for surface adsorption sites on six activated carbons. Microporous carbons were most affected by low molecular weight NOM because the high molecular weight NOM absorbs near the external carbon surface. However, the mesoporous carbons were impacted by a range of NOM molecules because NOM can access the entire structure of a more mesoporous carbon. One method of determining the concentration of directly competing compounds uses the equivalent background compound (EBC) theory, which

assumes an equivalent single compound to produce the differences observed between a distilled water isotherm and the target compound isotherm (Najm et al., 1991; 2002; Qi et al., 1994). This method can be used to predict the decreasing capacity of activated carbon for trace contaminants due to competitive adsorption of background organic matter.

2.3.2 NOM Effect on Membranes

NOM has also been shown to cause hydraulically irreversible fouling on membranes, mostly due to the hydrophilic characteristics of the NOM (Amy et al., 1999). Some studies have been done combining activated carbon and membranes hypothesizing that the activated carbon would absorb some of the NOM and result in less membrane fouling. Lee et al. (2000) found that the addition of PAC into feed water containing humic acids increased membrane fouling and decreased the flux, even though the PAC alone did not cause fouling. This could be due to the fact that there was more humic acid aggregation in the presence of PAC which caused more irreversible membrane fouling. Matsui et al. (2009) found that S-PAC alleviated long term trans-membrane pressure buildup by removing foulants that contributed to irreversible membrane fouling.

2.4 S-PAC Adsorption Capacity and Uptake Rate Modeling

Adsorption equilibrium can be modeled using either the Freundlich or Langmuir isotherm. However, these equations assume that the adsorption capacity of the activated carbon is independent of the carbon particle size. Matsui et al. used the Freundlich isotherm (Eq. 2.1) to describe the adsorption capacity changes with respect to the carbon particle size (2011). It was

assumed that K, the adsorption capacity parameter, increased with decreasing distance from the particle surface, which is a function of the particle radius, as follows:

$$q_E = K_f C_E^{1/n} \tag{2.1}$$

where C_E is the liquid-phase concentration of the trace contaminant (mg/L), q_E is the amount of trace contaminant adsorbed in the solid-phase in equilibrium with the liquid-phase concentration (mg/g), n is the Freundlich equilibrium parameter, and K_f is the Freundlich adsorption capacity parameter $(mg/g)(mg/L)^{1/n}$. A larger K_f represents a higher adsorption affinity, whereas a larger n demonstrates a more homogeneous surface of the adsorbent.

To simulate the dynamics of the adsorption process on activated carbon and to determine the diffusion coefficient (D_S) of a solute, the homogeneous surface diffusion model (HSDM) can be used. It predicts the diffusion of a molecule from the external surface of the carbon particle to the adsorption site (Baup et al., 2000). The HSDM model assumes that the particles of carbon are spherical, with uniformly distributed micropores that branch off of macropores undergoing radial mass transport (Matsui et al., 2009). This model can also be used to model desorption of trace contaminants, however it cannot be assumed that there is clean or virgin carbon, which is one of the assumptions used for modeling the adsorption processes (To et al., 2008b).

The partial differential equation for mass transport of the target compound within a spherical particle using the HSDM is:

$$\frac{\partial q}{\partial t} = \frac{D_s}{r^2}\frac{\partial}{\partial r}\left[r^2 \frac{\partial q}{\partial r}\right] \tag{2.2}$$

It is assumed that D_S is not concentration dependent, particle density is constant, and no reaction occurs between the solute and the particle (Qi et al., 1994).

A variable substitution, $u = qr$, converts Equation 2.2 to:

$$\frac{\partial u}{\partial t} = D_s \frac{\partial^2 u}{\partial r^2} \qquad (2.3)$$

Initial conditions for q and u are listed below. For desorption, a constant q_o, which is the initial solid phase concentration of a contaminant, across the particle radius is assumed. Adsorption with clean carbon is assumed when q_o is equal to 0.

$$q(r, t = 0) = q_o \quad \textit{For } 0 \le r \le R \qquad (2.4)$$

$$u(r, t = 0) = rq_o \quad \textit{For } 0 \le r \le R \qquad (2.5)$$

The boundary conditions for the center of the particle, r = 0, are:

$$\frac{\partial q}{\partial r}(r = 0, t) = 0 \qquad \textit{For } t > 0 \qquad (2.6)$$

$$u(r = 0) = qr = 0 \qquad \textit{For } t > 0 \qquad (2.7)$$

The Freundlich isotherm equation can then be used to describe adsorption equilibrium with respect to time (Equation 2.1). The HSDM equations are used to solve for the adsorbed concentration profile over time. The mass balance equation for a batch reactor, Equation 2.8, allows the bulk solution concentration profile to be found.

$$M_{tot} = \left(q_{avg}(t)C_c + C(t)\right)V \qquad (2.8)$$

2.5 Desorption of Trace Contaminants and NOM from Activated Carbon

Desorption of trace contaminants can occur in real systems when the adsorbent residence time is much longer than the hydraulic residence time (To et al., 2008b). The two types of desorption to consider are displaced desorption and non-displaced desorption. Displaced desorption occurs from competition for adsorption sites from strongly competing matter and nondisplaced desorption occurs from a decrease in the bulk solution contaminant

concentration. In a GAC or fixed bed absorber system, the desorption of trace contaminants from activated carbon could become a problem when the carbon residence time in an absorber is greater than the hydraulic residence time or when the absorber influent concentration of a pollutant drops. Displaced desorption could also occur in a GAC or fixed bed absorber when there is a continuous supply of new strongly competing compounds that are constantly displacing the previously adsorbed contaminants. This occurrence would lead to a shorter adsorbent life and a higher cost of treating water (To et al., 2008b). The desorption of trace contaminants from S-PAC particles has yet to be studied, however in a real system this would not be an issue. These desorption results are studied instead to help further characterize S-PAC particles by understanding more about their physical and chemical properties.

Thacker et al. (1983) investigated adsorption and desorption in a GAC column and was able to observe the displaced desorption of pre-adsorbed dichlorophenol when dimethylphenol, a strongly competing contaminant, was introduced. The HSDM model was used to predict these step changes in the influent concentration to a GAC bed. Luft used a bench scale GAC column to show that chloroform, a weakly adsorbing compound, was easily displaced by TCE, a strongly adsorbing compound. For a period of time after the TCE was introduced into the system, the effluent chloroform concentration was higher than the influent concentration while the effluent TCE concentration was lower than the influent concentration, meaning that the TCE was staying in the system (Crittenden et al., 1985; Luft, 1984). Corwin & Summers (2011) also found that desorption from GAC absorbers was occurring, but at very low concentrations. It was concluded that pore blockage or hindered back diffusion caused by irreversibly adsorbed dissolved organic matter on the GAC surface could be responsible for these slow kinetics.

To et al. (2008a, 2008b) studied the desorption kinetics of trace contaminants on PAC and showed that strongly competing compounds that are similar in size to trace contaminants and directly compete for the carbon surface without causing pore blockage, decreased the surface sites available on the carbon for the surface diffusion of trace contaminants and enhanced desorption through the displacement of these trace contaminants. In contrast, pore-blocking background organic matter, which is larger in size than trace contaminants, was found to be useful in preventing trace contaminant desorption by reducing the rate of release of the trace contaminants that were already preloaded on to the PAC. Pore-blocking compounds can also hinder the uptake of strongly competing compounds, which would prevent the displacement of already adsorbed trace contaminants (Li et al., 2003).

The HSDM has been used in previous studies to find effective adsorption and desorption diffusion coefficients in systems with strongly competing compounds. To et al. (2008) found that the diffusion coefficient increased as the strongly competing matter concentration increased, which shows a shift from surface diffusion to pore diffusion as the preferred adsorption sites were occupied. This model can be used to elucidate the effect of surface competition during desorption on activated carbons.

3 RESEARCH OBJECTIVES

The main motivation for this work is to improve our understanding of the characteristics of S-PAC. Specifically, this research project focused on two objectives.

1. ***Measure the desorption kinetics of trace contaminants on S-PAC when in competition with a strongly competing compound.*** This goal was achieved by using radiolabeled atrazine as a trace contaminant and p-DCB (1,4-dichlorobenzene) as a strongly competing compound. Because of their size similarities, p-DCB and atrazine were expected to be able to access the same adsorption sites on activated carbon particles. However, the compound structure and chemistry will also affect the competition between p-DCB and atrazine. Atrazine is an aromatic, hydrophilic compound and p-DCB is an aromatic, hydrophobic compound. It has been found that aromatic hydrophobic compounds will absorb more strongly to activated carbon than aromatic hydrophilic compounds (Nam et al., 2014; Quinlivan et al., 2005; Ren et al., 2016; Snyder et al., 2007). It was also expected that trace contaminants would adsorb deeper into the PAC particles than the S-PAC particles and therefore would desorb at a slower rate.
2. ***Measure the desorption kinetics of trace contaminants on S-PAC when in competition with a pore blocking organic compound and a strongly competing compound.*** This goal was achieved by using Suwannee River NOM (SRNOM) as a model pore-blocking compound, p-DCB as a model strongly competing compound, and radiolabeled atrazine as a model trace contaminant. SRNOM has particles that are much larger in size than p-DCB and atrazine, therefore it was expected to cause pore-blockage on the PAC and S-PAC particles. It was also suspected that by blocking these adsorption sites, the large

molecular weight SRNOM would slow the rate of trace contaminant desorption. However, the S-PAC has more external surface area than the PAC, so the SRNOM is expected to block fewer pores on the S-PAC and slow trace contaminant desorption less than it would on the PAC.

4 MATERIALS AND METHODS

4.1 Adsorbents

Two commercially available activated carbon materials were chosen; Water Carb 800 and Aqua Nuchar. In order to compare carbon characteristics, four different sizes of S-PAC for each of these activated carbons were tested, along with the parent PAC material. The S-PAC was produced using a wet bead mill containing 0.3 – 0.5 mm yttrium-stabilized zirconia oxide ceramic beads (Partlan et al., 2016). A stock solution of 2000 mg/L in distilled deionized water (DDI) was prepared for each size adsorbent.

Water Carb 800 (WC800) (Standard Purification) is a commercially available bituminous coal based activated carbon that was used as one of the adsorbent materials. In addition to the PAC, milling times of 1 pass, 30 minutes, 1 hour, and 6 hours were used.

Aqua Nuchar (Mead Westvaco), a wood based activated carbon, was the other adsorbent material that was chosen. In addition to the PAC, S-PAC with milling times of 1 pass, 20 minutes, 1 hour, and 6 hours were used. A 20 minute milling time was selected for the Aqua Nuchar because there was no 30 minute milling time available in our lab.

4.1.1 Properties of Adsorbents

The properties of WC800 and Aqua Nuchar are shown in **Table 4.1**, **Table 4.2**, and **Table 4.3**. The Aqua Nuchar parent PAC material has a higher specific surface area and a higher specific pore volume than the WC800 parent PAC material. There is no correlation between milling time and specific surface area for the WC800 but as the milling time increases the specific surface

area of the Aqua Nuchar decreases. Images of PAC and all S-PACs from the WC800 carbon were taken by scanning electron microscopy (SEM) at 5,000 times magnification reveal the range of particle sizes from large PAC and 1 pass particles to small 30 minute, 1 hour, and 6 hour particles. The particles visibly decrease in size from the PAC to the 6 hour particles and can be seen below in **Figure 4.1**.

Table 4.1 Measured characteristics of parent PAC materials: specific surface area and total pore volume (Partlan et al., 2016).

Origin Material	Label	Product Name	PAC Size (μm)	Specific Surface Area (m^2/g)	Specific Pore Volume (cm^3/g)
Bituminous Coal	WC800	Watercarb-800	12.3	644	0.35
Wood	WD	Aqua Nuchar	11.3	1676	0.89

Table 4.2 Particle size, surface area, and pore volume measurements for WC800 and Aqua Nuchar (Partlan et al., 2016).

Carbon	Particle Size (nm)	Specific Surface Area (m^2/g)	Total Pore Volume (cm^3/g)	Macropore Volume (cm^3/g)	Mesopore Volume (cm^3/g)	Sub-micropore Volume (cm^3/g)	Primary Micropore Volume (cm^3/g)
WC800							
PAC	12300	644	0.35	0.04	0.09	0.08	0.14
1 pass	628	777	0.44	0.05	0.13	0.08	0.18
30 min	398	857	0.49	0.07	0.13	0.09	0.20
1 hr	329	872	0.35	0.10	0.09	0.12	0.04
6 hrs	230	762	0.69	0.11	0.33	0.10	0.15
Aqua Nuchar							
PAC	11300	1676	0.89	0.03	0.49	0.37	0.00
1 pass	1183	1642	1.05	0.05	0.68	0.32	0.00
20 min	590	1521	0.91	0.06	0.55	0.29	0.02
1 hr	491	1269	0.89	0.13	0.45	0.23	0.09
6 hrs	440	1008	0.84	0.28	0.29	0.25	0.02

Macropore (> 50 nm); mesopore (2–50 nm); submicropore (1–2 nm); primary micropore (> 1 nm)

Table 4.3 Surface charge properties measured by point of zero charge, isoelectric point, and percent oxygen content. The difference between pH_{PZC} and pH_{IEP} is shown as ΔpH. Carbons are distinguished by material and milling time. Dashed lines indicate that measurements were not taken (Partlan et al., 2016).

Carbon	pHpzc	pH_{IEP}	ΔpH	Oxygen Content (w/w%)	Carbon	pHpzc	pH_{IEP}	ΔpH	Oxygen Content (w/w%)
BC1					**WD**				
PAC	10.37	--	--	2.41	PAC	6.2	--	--	7.14
1 pass	9.31	3.27	6.04	2.79	1 pass	6.25	2.48	3.77	7.25
30 mins	8.92	2.71	6.21	4.19	20 mins	5.82	3.06	2.76	8.3
1 hr	8.07	2.57	5.5	5.23	1 hr	5.11	2.67	2.44	9.15
6 hrs	7.75	2.64	5.11	7.86	6 hrs	4.95	2.84	2.11	10.5

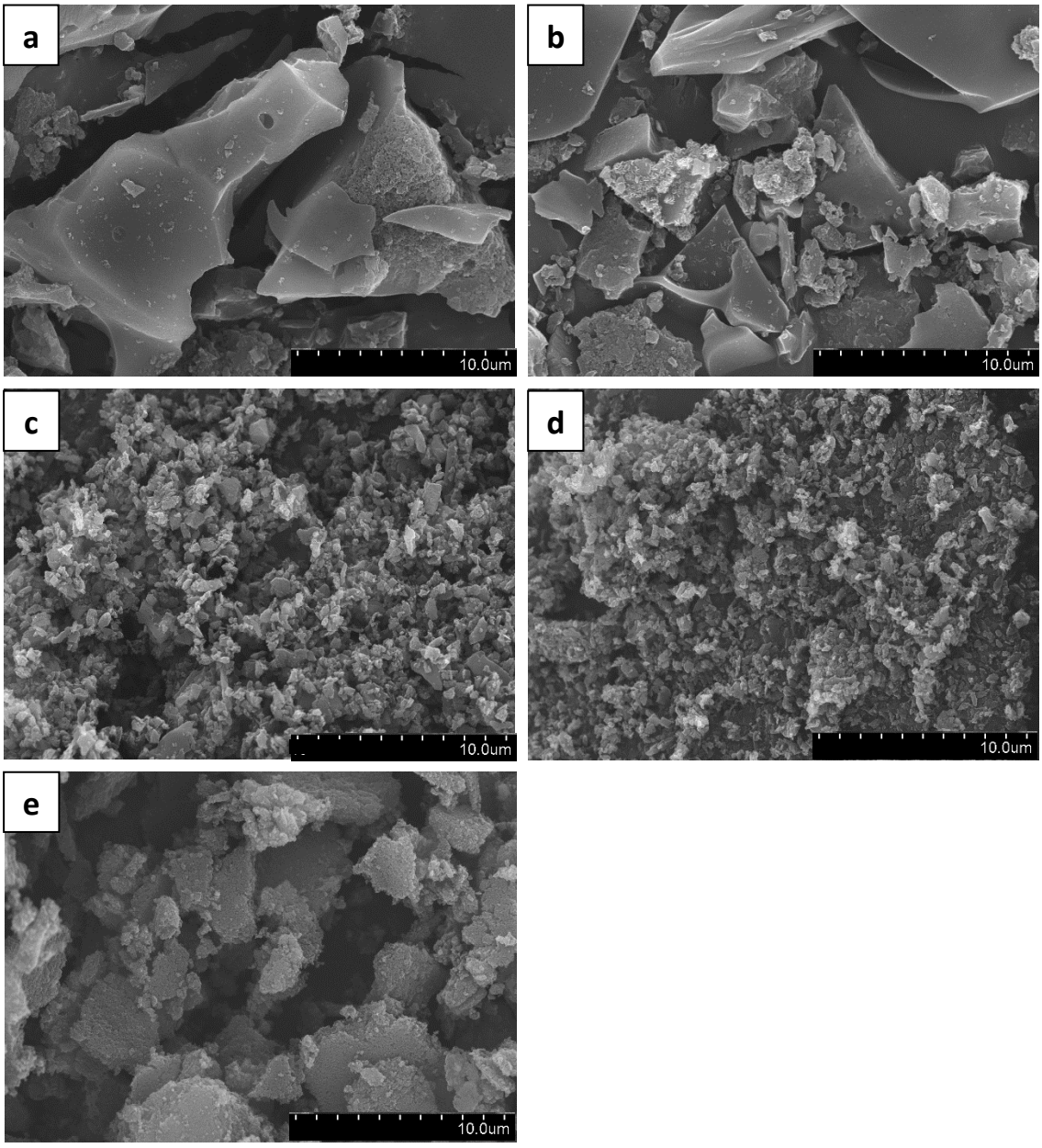

Figure 4.1 Scanning electron microscopy images (5K magnification) of WC800 (a) PAC, (b) 1 Pass, (c) 30 minutes, (d) 1 hour and (e) 6 hours.

Partlan et al. determined the material characteristics and characterization methods for these PACs and S-PACs (2016). For particles that were smaller than 6 µm, size distributions were

determined by dynamic light scattering (DLS) and particles larger than 6 μm were measured by an optical microscope with a 40x objective lens. The surface area was calculated with the Brunauer-Emmett-Teller (BET) equation, using the N_2 physisorption data at 77K. It was found that the mean particle size decreased with longer milling time for each of the carbons that were used. It was also determined that Aqua Nuchar, the wood based carbon, had the largest mean particle size at 440 nm and the largest resistance to milling.

4.2 Adsorbates

Two types of adsorbates were chosen as model contaminants for this study, atrazine and 1,4-Dichlorobenzene (p-DCB).

4.2.1 Atrazine

Atrazine is a compound that has been used as an herbicide and is one of the most prevalent trace contaminants in ground and surface waters in the United States. It was chosen as a model compound because it is expected to behave in a similar way to many other aromatic compounds during the adsorption process onto activated carbon and because several previous adsorption studies have used it, so data the can be compared directly.

Radiolabeled 14C-atrazine (American Radiolabeled Chemicals, Inc) with a specific radioactivity of 160 mCi/mmol was used as the model trace contaminant in this study. The molecular weight of atrazine is 215.7 g/mol and the structure of atrazine can be seen below in **Figure 4.2** Molecular structures of atrazine (a) and 1,4-dichlorobenzene (b).. Some other various chemical and physical properties are listed in **Table 4.4.**

Atrazine desorption was detectable using a 1:300 ratio of radiolabeled atrazine to non-radiolabeled atrazine. A non-labeled atrazine stock solution was made of 100 mg/L in ethanol and a labeled atrazine stock solution was made of 1.34 mg/L in ethanol. Both of these stock solutions were stored at -18°C.

Samples were measured with a liquid scintillation counter (LSC) (Tri-Carb B2910TR, PerkinElmer) to determine the atrazine concentration in each sample. Each LSC measurement vial contained 2.5 mL of sample and 18 mL of scintillation cocktail (UltimaGold XR). The count time was 15 minutes per sample. LSC measures radioactivity of a sample by counting the electrical pulses that are detected by a photomultiplier tube. This is accomplished by mixing the active material with a liquid scintillator, and counting the resultant photon emissions (Lowe et al., 1962).

4.2.2 1,4-Dichlorobenzene

P-DCB (Sigma Aldrich) was used to represent the strongly competing compound for these experiments. P-DCB is an aromatic, hydrophobic compound that is mainly used as a pesticide and a deodorant. The molecular weight is 147 g/mol, which is similar in size to atrazine. Since the size of p-DCB and atrazine are similar, P-DCB competes directly with atrazine for adsorption sites and does not cause pore blockage on the activated carbon. The structure of p-DCB can be seen below in **Figure 4.2**. Some other various chemical and physical properties are listed in **Table 4.4.**

For these experiments, a p-DCB stock solution was made of 10,000 mg/L in methanol and stored at a temperature of 4°C.

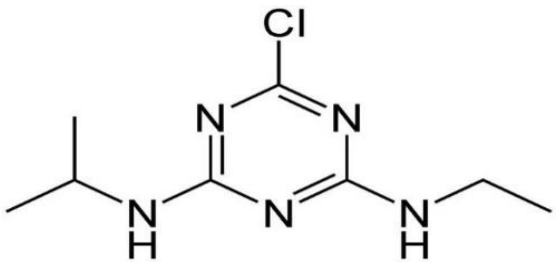

a.

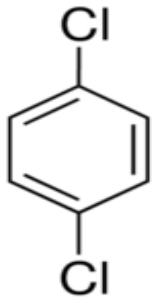

b.

Figure 4.2 Molecular structures of atrazine (a) and 1,4-dichlorobenzene (b).

Table 4.4 Adsorbate Properties

Compound	**Atrazine**	**1,4-dichlorobenzene**
Chemical Formula	$C_8H_{14}ClN_5$	$C_6H_4Cl_2$
Dimensions (Å)	9.6 x 8.4 x 3[a]	6.7 x 5.5 x 1.8[i]
MW (g/mol)	215.7	147
Molecular Volume[b] (m^3/kmol)	0.247	0.113[c]
pK_a	1.95[d]	-
Solubility in Water (g/L)	0.03[e]	0.08[g]
log K_{ow}	2.75[e]	3.44[h]

[a](Pelekani et al., 2000); [b]Estimated using the Le Bas method; [c]Molecular volume for 1,2-dichlorobenzene (Ran et al., 2003); [d](Colombini et al., 1998); [e](USEPA, 2015); [g](Yalkowsky et al., 2003); [h](Hansch et al., 1995); [i]Estimated using bond lengths and atomic radii.

4.2.3 Suwanee River Natural Organic Matter

Suwanee River NOM (SRNOM) (RO Isolation) was obtained from the International Humic Substances Society (St. Paul, MN) and was used to represent the pore-blocking material in these experiments. A stock solution of approximately 80 mg/L as organic carbon dissolved in ultrapure water was prepared and stored at a temperature of 4°C.

4.3 Displaced Desorption Experiments from Strongly Competing Adsorbates

The steps in these experiments were to preload and equilibrate the PAC and S-PAC with atrazine, and then to add p-DCP and measure the desorption rate of the atrazine. These tests were performed in 2-liter media bottles with a carbon concentration of 5 mg/L so that when samples were taken, it would not deplete the overall carbon concentration in the reactor significantly. The background solution was DDI water that was pH adjusted to 7 using a 1 mM phosphate buffer.

First, fresh PAC and S-PAC of 5 mg/L was preloaded with atrazine (100 ug/L) and placed on a rotary tumbler. Atrazine concentration was measured on day 7 to check for equilibrium and ensure that the adsorption capacity of the carbon was reached. On day 7, p-DCB (2 mg/L) was added to displace the atrazine. The solution was placed on a stir plate and atrazine desorption was monitored over 420 minutes. More frequent samples were taken at the beginning to capture the more rapid changes in concentration.

A two port sampling cap was used to seal the media bottles because p-DCB is a volatile compound. A 1.6 liter Tedlar PVF gas sampling bag (Saint-Gobain Chemware) filled with nitrogen gas was connected to one port to replenish the sampled volume and the headspace in the bottle was minimized to prevent p-DCB volatilization. A tube was connected to the other port that remained closed, except for when samples were being removed from the bottle. A diagram and a picture of this experimental setup can be seen below in **Figure 4.3** and **Figure 4.4**.

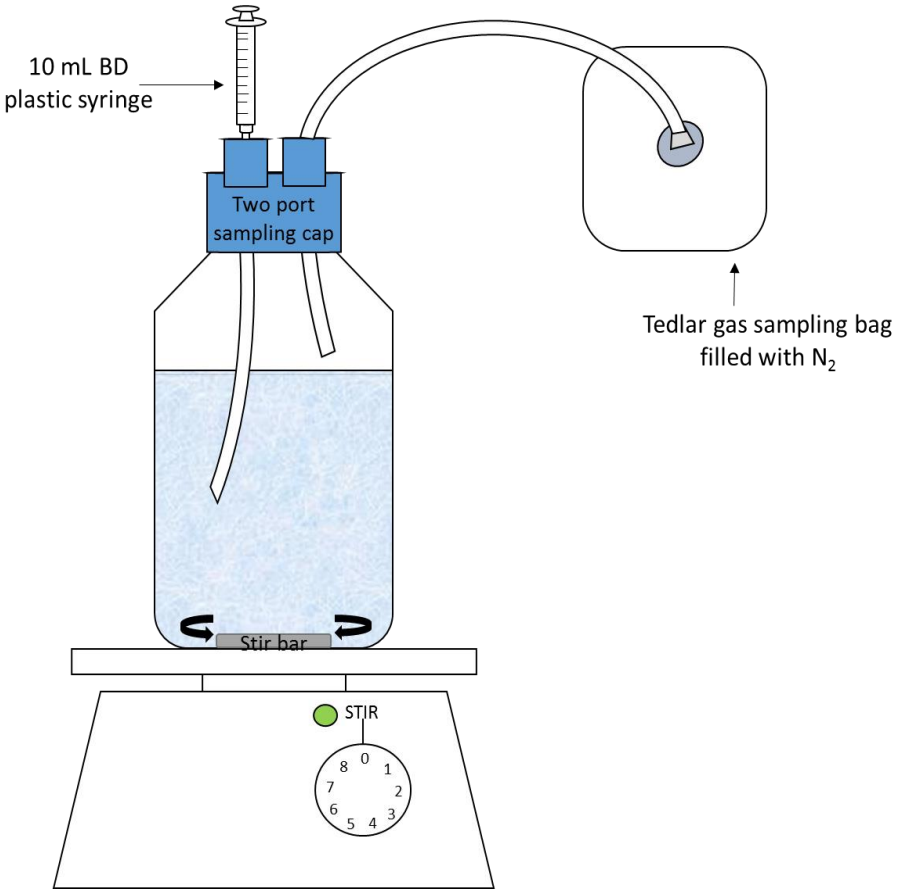

Figure 4.3 Experimental setup diagram for the displaced desorption experiments

Figure 4.4 Experimental setup picture for the displaced desorption experiments.

All collected samples were filtered through a 0.1 micron polyvinylidene difluoride (PVDF) hydrophilic membrane (Millipore VVLP) using a syringe filter to remove the PAC and S-PAC. All membranes were soaked in DDI water overnight before use. This method was chosen over centrifugation of the carbon because it was quicker and allowed for an analysis of the early desorption kinetics in each experiment. A control experiment with only atrazine and DDI water was filtered through a PVDF membrane to determine how much atrazine was lost due to filtration. The solution was then tumbled for 7 days and filtered again to determine if there was a loss in atrazine within the system after being in the glass media bottle for 7 days. The data can be seen below in **Table 4.5**. Approximately 3% of atrazine was removed on average from the

system due to filtration and approximately 2% was lost in the system after 7 days of being placed on a rotary tumbler.

Table 4.5 Control experiment to determine how much atrazine was lost due to filtration and being placed on a rotary tumbler for 7 days.

Control Solution		Filtered Solution		Tumbled 7 days		Tumbled 7 days and filtered	
Sample	**Conc. (µg/L)**	**Sample**	**Conc. (µg/L)**	**Sample**	**Conc. (µg/L)**	**Sample**	**Conc. (µg/L)**
1	99.55	1	95.56	1	97.40	1	94.11
2	97.78	2	94.99	2	96.51	2	95.75

For analysis of the atrazine, samples of 2.5 mL were combined with 18 mL of liquid scintillation cocktail. The samples were then analyzed using a liquid scintillation counter to measure the radioactivity of the sample. This experiment was repeated using each of the milling times selected above for the WC800 and the Aqua Nuchar. Another set of the same experiments was also completed for repetition to ensure that everything was working properly and to check that the results were consistent. Some examples of these repeat experiments can be seen in **Appendix 7.1** in **Figure 7.1** and **Figure 7.2**.

4.4 Displaced Desorption Experiments from Strongly Competing and Pore-Blocking Organic Matter Combined

This experiment was done in the same way as the previous experiment, with the addition of preloading SRNOM on the carbon as well as atrazine. First, fresh PAC and S-PAC of 5 mg/L was preloaded with atrazine (100 ug/L) and placed on a rotary tumbler. On day 4, SRNOM was added to each bottle to obtain an initial concentration of 4 mg/L. This sequential adsorption mimics the situation in which influent pore-blocking NOM adsorbs after the uptake of the target contaminant in a packed-bed absorber column. Even though this is not typically how S-PAC

would be applied in a real system, this experimental design will help us understand how competition from SRNOM affects atrazine adsorption and desorption on S-PAC in general. Atrazine concentration was measured on day 12 to check for equilibrium and then p-DCB (2 mg/L) was added to displace the atrazine. The solution was placed on a stir plate and atrazine desorption was monitored over 420 minutes. More frequent samples were taken at the beginning to capture the more rapid changes in concentration.

The sampling procedure and analytical methods were the same procedures and methods that was used for the displaced desorption experiments with only strongly competing matter. This experiment was repeated using each of the milling times stated above for the WC800 and the Aqua Nuchar. Another set of the same experiments was also completed for repetition to ensure that everything was working properly and to check that the results were consistent.

5 RESULTS AND DISCUSSION

5.1 Objective 1 – Strongly Competing Compound Only

5.1.1 WC800

p-DCB was used as a strongly competing compound and atrazine was used as the trace contaminant SOC in order to determine the desorption kinetics of trace contaminants on PAC and S-PAC due to competition from a strongly competing compound. The p-DCB competes for the same sites on the activated carbon as the atrazine, which can displace the atrazine that has already been adsorbed.

The full set of data (420 minute experiment) for the competition from strongly competing matter on WC800 is shown in **Figure 5.1** with an inset showing a closer view of the initial desorption data. The data points shown are the average atrazine concentration between two data sets of the same experiment to check for repeatability. The atrazine desorbed the slowest from the PAC, which was expected because the PAC particles have less specific external surface area than the S-PAC particles. After the PAC, the S-PAC 1 pass was the next slowest to desorb from the WC800. The 30 minute, 1 hour, and 6 hour milling times did not show a clear trend in desorption kinetics. It is suspected that the desorption kinetics after the 1 pass milling time are happening so fast that they could not be seen using the experimental design from above.

The particle size of WC800 PAC was 12,300 nm while the particle size of the WC800 1 Pass was 628 nm. With just one pass through the mill, the particle size was decreased by over 90% of its original size. The particle sizes of the WC800 30 minute milling time, 1 hour milling time and 6

hour milling time were 398 nm, 329 nm and 230 nm, respectively. These data show that the particle sizes did not decrease as drastically after 30 minutes of milling and supports the desorption results shown in **Figure 5.1**. These results are also supported by Partlan et al. (2016), who found that one pass through the mill resulted in particle sizes near or below one micrometer and further milling continued to reduce median particle sizes but with diminishing returns, and by Amaral et al. (2016), who found that atrazine adsorption increased from as little as 20% up to 99% between the PAC and S-PAC for different types of carbon, but correlated less among the different S-PACs. This could also be a result of the carbon milling method that was used to make the S-PACs. Using a different technique for milling with different size beads could crush the carbon differently and result in more distinguishable difference between milling times.

It can also be seen in **Figure 5.1** that there is a faster initial release of atrazine that is adsorbed to the external surfaces of the carbon followed by a slower release that continues to increase. This increasing slope in the atrazine concentration could be caused by the slow release of atrazine from the internal pores of the carbon. Even though there are more internal pores on the PAC, it is believed that there are still some internal pores on the S-PAC as well.

The increasing slope in the atrazine concentration could also be caused by a longer-term competition between atrazine and p-DCB. Once the atrazine is displaced it from the carbon, it is then available to re-adsorb to another adsorption site. This process could continue causing a slowly increasing atrazine concentration in the solution as atrazine is displaced and reabsorbed to different sites on the carbon where it can then become displaced again.

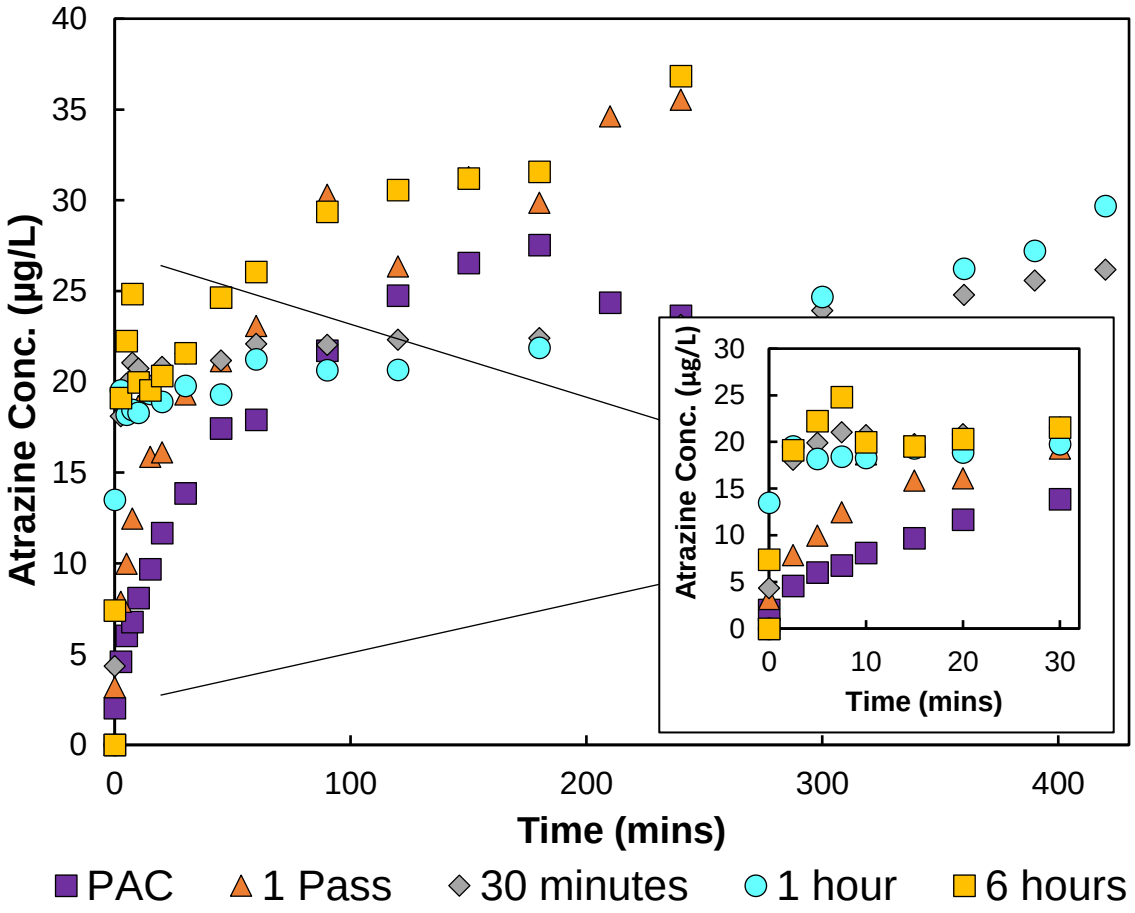

Figure 5.1 Average desorption kinetics of atrazine on WC800 using p-DCB only for PAC, 1 Pass, 30 minutes, 1 hour and 6 hour milling times over a 420 minute time span with an inset of the initial desorption kinetics.

The desorption rates of the WC800 and Aqua Nuchar PAC and S-PACs with competition from strongly competing matter only were estimated by fitting a kinetic desorption equation through the data, which is shown in **Equation 5.1,** where k is the desorption rate of the atrazine that is being displaced from the activated carbon, C_o is the final concentration of atrazine that was desorbed from the carbon, and C is the concentration of atrazine at a specified time.

$$C = C_o - C_o * e^{-k*time} \qquad (5.1)$$

Examples of the input equations and output data can be found in **Appendix 7.3**. The estimated desorption rates, k, for each carbon type and milling time can be seen in **Table 5.1**.

Table 5.1 Desorption rate for WC800 and Aqua Nuchar with competition from strongly competing matter only, determined by fitting a kinetic desorption equation through the data. The goodness of fit (R-Square) value from the model is also reported.

Carbon	Desorption Rate, k (min^{-1})	R-square	Carbon	Desorption Rate, k (min^{-1})	R-square
WC800			**Aqua Nuchar**		
PAC	0.0229	0.97	PAC	0.0236	0.95
1 pass	0.0860	0.90	1 pass	0.0901	0.81
30 mins	0.6945	0.96	20 mins	1.2580	0.86
1 hr	1.6200	0.95	1 hr	0.2708	0.67
6 hrs	0.4275	0.73	6 hrs	0.1366	0.73

The PAC for both types of carbon had the slowest desorption rate which was then followed by the 1 pass which had the next slowest desorption rate. In order to understand the reasons for the differences in desorption rates, the particle size, specific external surface area, and other properties were considered. In previous work by others, a multiple linear regression analysis was performed to compare the various properties to atrazine removal in membrane coating experiments. The specific external surface area proved to be the best predictor of atrazine removal while oxygen content was found to be the next best predictor (Amaral et al., 2016). The specific external surface area of WC800 went from 0.24 m^2/g on the PAC to 4.78 m^2/g on the 1 pass and 12 m^2/g on the 6 hour milling time. There was a significant increase in the specific external surface area when going from PAC to 1 pass but the increase was less significant for longer milling times. Those membrane-experiment adsorption results support the desorption data shown in **Figure 5.1** since the PAC and 1 pass had the slowest desorption

kinetics followed by the 1 pass. This is also supported by the desorption kinetic results shown in **Table 5.1** where PAC was the slowest followed by 1 pass for both types of carbon.

The desorption rates shown in **Table 5.1** for WC800 using the kinetic desorption equation increased with milling time until the 6 hour milling time was reached. This suggest that there could be a peak milling time for WC800 carbon. Once the carbon is milled for too long, it is suspected that the pores become crushed and this has an effect of the desorption rate of atrazine from the carbon. The estimated desorption rates as a function of milling time can be seen in **Figure 5.2**. The desorption rates increased linearly with milling time until the 6 hour milling time was reached, which is considered to be an outlier within the data. These desorption rates are also consistent with Amaral et al. (2016) who showed that atrazine removal increased with milling time reaching approximately 80% removal, except for the WC800 6 hours which only removed approximately 60% of atrazine.

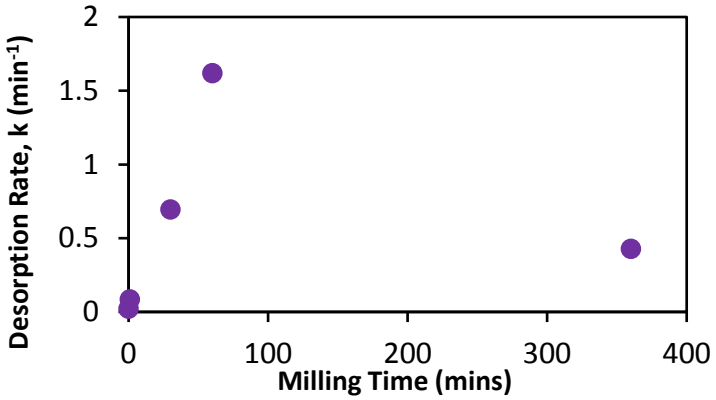

Figure 5.2 Desorption rate as a function of milling time for WC800 carbon.

Partlan et al. found that the oxygen content correlated with milling time and an increased specific external surface area, because the majority of new oxygen is attached to the external surfaces only (2016). The oxygen content of the WC800 PAC was 2.41% while the oxygen content of the WC800 1 pass was 2.79%. The oxygen content of the WC800 30 minutes, 1 hour and 6 hours were 4.19%, 5.23% and 7.86%, respectively. The estimated desorption rate of the PAC and all S-PACs for WC800 were also plotted against the oxygen content, pH_{PZC}, and pH_{IEP} which can be seen in **Figure 5.3**. It was determined that oxygen content does not affect the desorption rate of atrazine from WC800 carbon.

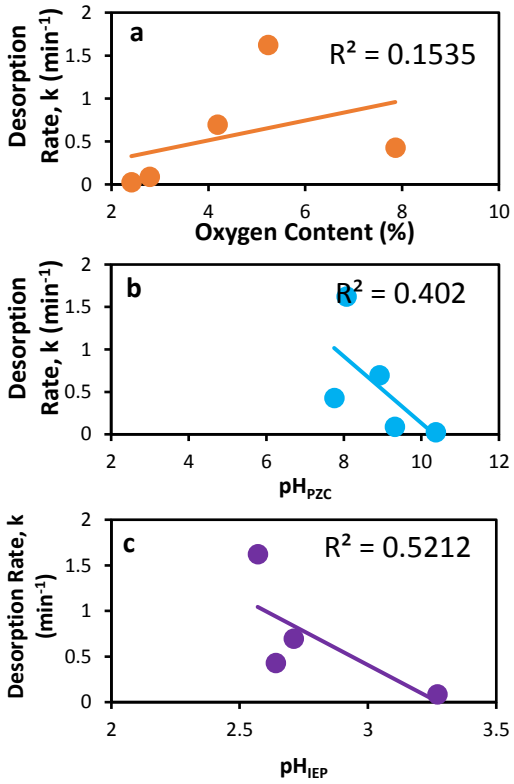

Figure 5.3 Correlations between the estimated desorption rate for WC800 and (a) oxygen content, (b) pH_{PZC}, and (c) pH_{IEP}.

5.1.2 Aqua Nuchar

The full set of data (420 minute experiment) for the competition from strongly competing matter on Aqua Nuchar can be seen below in **Figure 5.4** with an inset showing a closer view of the initial desorption kinetics. The data points shown are the average atrazine concentration between two data sets of the same experiment to check for repeatability. The PAC was the slowest to desorb on the Aqua Nuchar carbon as well, which is what was expected due to the smaller amount of specific external surface area on the PAC particles when compared to the S-PAC particles. The 1 pass milling time had the next slowest desorption kinetics, even though there is not as clear of a trend as was shown on the WC800 carbon. This is followed by the 20 minute, 1 hour, and 6 hour milling times, with no clear trend in desorption kinetics between the last three. It is suspected that the desorption kinetics after the 1 pass milling time are happening so fast that they could not be seen using the experimental design from above. According to Amaral et al., the Aqua Nuchar carbon showed no correlation between milling time and atrazine removal even though the wood based carbon had the highest surface area and the largest change with milling time. The highest atrazine removal for Aqua Nuchar was obtained with the 10 minute milling time and the 20 minute milling time at 58% and 55%, respectively, while the lowest atrazine removal was found with the 5 minute milling time at 18% (2016). This is consistent with the desorption data shown in **Figure 5.4**. The 20 minute milling time had a higher initial desorption capacity than any of the other milling times. This is also consistent with the desorption rates found in **Table 5.1** for Aqua Nuchar, showing that the 20 minute milling time had the highest desorption rate. There was no correlation between the 1 pass, 1 hour and

6 hour milling times with respect to desorption kinetics or capacity, which could be due to the initial kinetics occurring too fast to be measured using the experimental design from above.

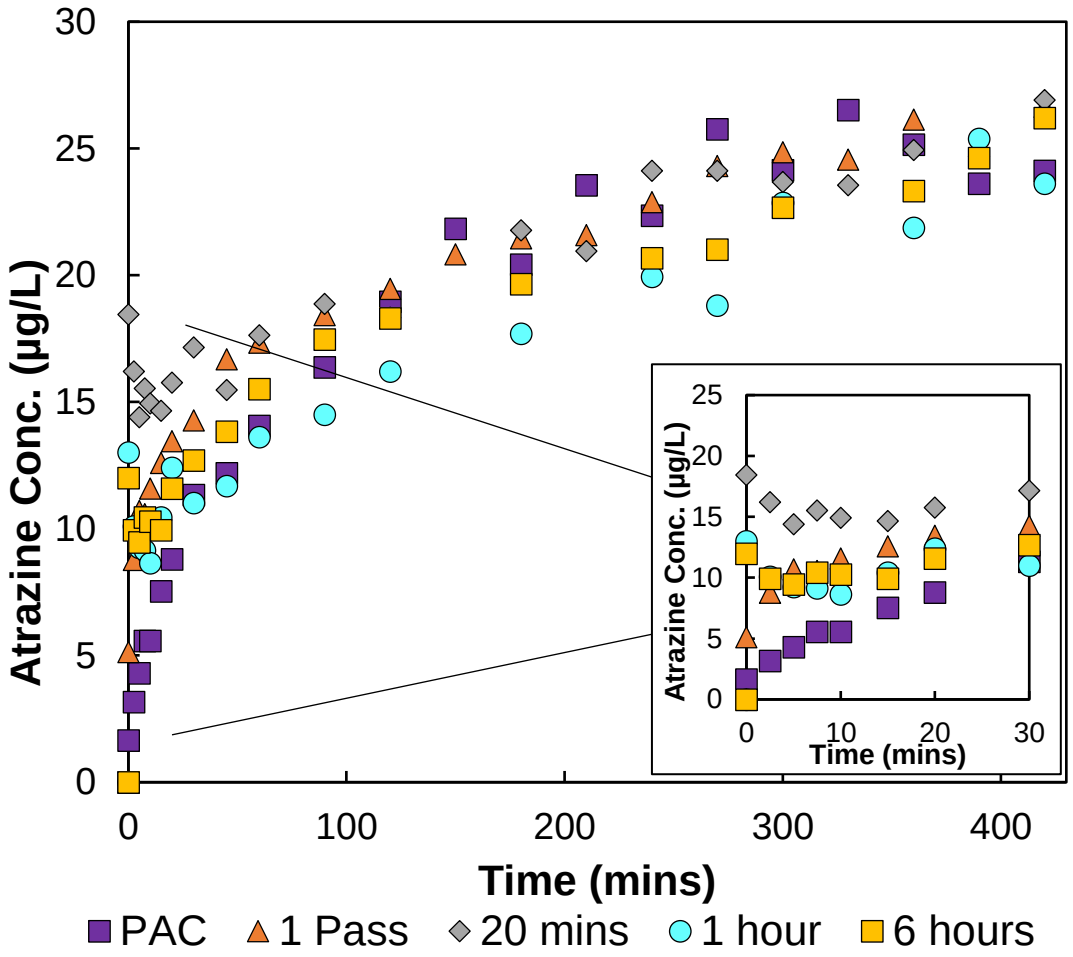

Figure 5.4 Average desorption kinetics of atrazine on Aqua Nuchar using p-DCB only for PAC, 1 Pass, 30 minutes, 1 hour and 6 hour milling times over a 430 minute time span with an inset of the initial desorption kinetics.

The particle size of the Aqua Nuchar carbon decreased with milling time going from a PAC size of 11,300 nm to a 1 pass size of 1183 nm and a 6 hour size of 440 nm. The difference between the PAC particle size and the 1 pass particle size is very large which could explain why the PAC desorption kinetics are noticeably slower than the S-PAC kinetics. After the 1 pass

milling time, the trend between desorption kinetics becomes less clear which is supported by the smaller decrease in particle size as a function of milling after 1 pass.

The estimated desorption rates shown in **Table 5.1** for Aqua Nuchar using the kinetic desorption equation increased with milling time until the 1 hour milling time was reached. This suggest that there could be a peak milling time for the Aqua Nuchar carbon as well. The estimated desorption rates as a function of milling time can be seen in **Figure 5.5**.The desorption rates increas linearly with milling time until the 1 hour milling time is reached, and then begin to decreas from the 1 hour to the 6 hour milling time.

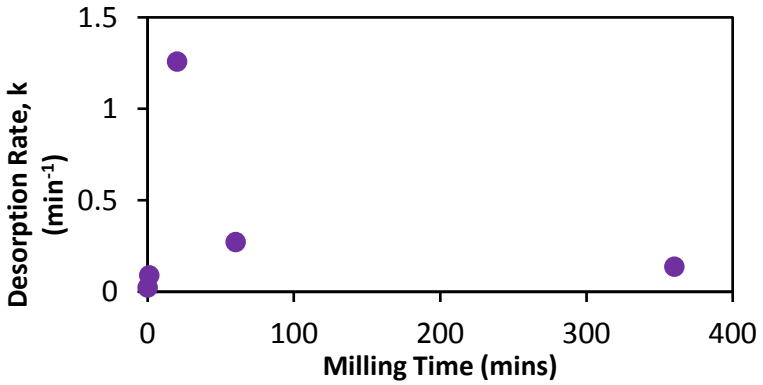

Figure 5.5 Desorption rate as a function of milling time for Aqua Nuchar carbon.

As milling time increased, the pH_{PZC} of all carbons decreased and the oxygen content of all carbons increased, which is shown in **Table 4.3**. Dunn and Knappe also reported an increase in oxygen content and a decrease in pH_{PZC} with increased milling time (2013). The pH_{PZC} indicates the acidity/basicity of an activated carbon and can alter the preferential adsorption with respect to the adsorbate charge (Dastgheib et al., 2004). The pH_{IEP} of either carbon sample did not change with milling time or correlate with oxygen increases. This could be because the outer

surface is easily oxidized which lowers the pH_{PZC} (Partlan et al., 2016). The oxygen content of Aqua Nuchar did not correlate with an increase in milling time between the PAC and the 1 pass. However, the trend can be seen after one pass through the mill. The PAC had an oxygen content of 7.14% while the 1 pass, 20 minutes, 1 hour and 6 hours had oxygen contents of 7.25%, 8.30%, 9.15% and 10.50%, respectively. The desorption rate of the PAC and all S-PACs were plotted against the oxygen content, pH_{PZC}, and pH_{IEP} which is shown in **Figure 5.6**. It was determined that oxygen content does not have an effect on the desorption rate of atrazine from activated carbon.

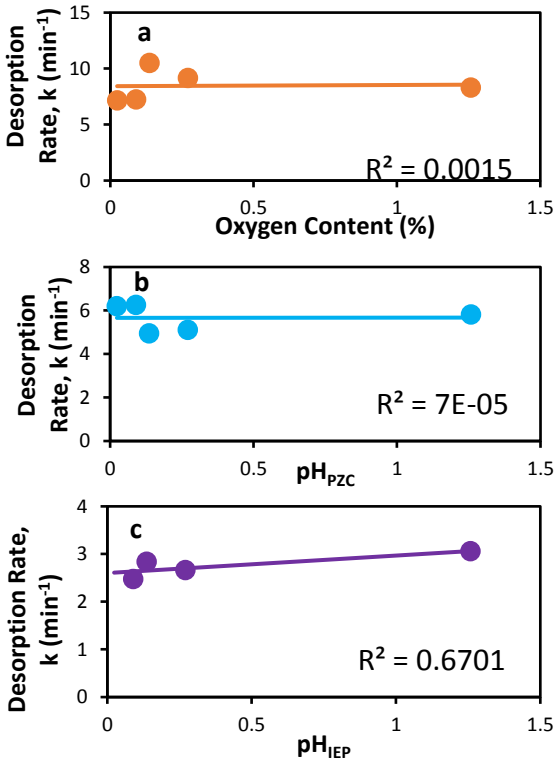

Figure 5.6 Correlation between the estimated desorption rate for Aqua Nuchar and (a) oxygen content, (b) pH_{PZC}, and (c) pH_{IEP}.

5.2 Objective 2 – A Strongly Competing Compound and Pore Blocking Organic Matter

When measuring the desorption kinetics on PAC and S-PAC from competition between a pore blocking organic compound, a strongly competing compound and the trace contaminant SOC, SRNOM was used as a pore blocking organic compound, p-DCB was used as a strongly competing compound and atrazine was used as the trace contaminant SOC. The p-DCB competes for the same sites on the activated carbon as the atrazine, which can displace the atrazine that has already been adsorbed. The SRNOM adsorbs to the external surfaces and large diameter pores of PAC and S-PAC which can block the adsorption of trace contaminants on-to the carbon and also stop the displacement of trace contaminants that are pre-adsorbed on the carbon.

It was expected that the SRNOM would block the desorption of the pre-adsorbed atrazine from the pores on the activated carbon, and therefore the desorption kinetics would be slower with SRNOM than when there was no SRNOM present in the water. **Figure 5.8** and **Figure 5.9** show the desorption kinetics of atrazine on (a) WC800 PAC (b) WC800 1 Pass (c) WC800 30 minutes (d) WC800 1 hour (e) WC800 6 hours (f) Aqua Nuchar PAC (g) Aqua Nuchar 1 Pass (h) Aqua Nuchar 20 minutes (i) Aqua Nuchar 1 hour and (j) Aqua Nuchar 6 hours all with and without SRNOM. To more clearly observe differences in kinetics, the first 30 minutes are shown separately in **Figure 5.9**. Repeats for each data set were completed and shown in **Figure 5.8** and **Figure 5.9** as the circle and square outlines.

The WC800 PAC is shown in **Figure 5.8 (a)** and **Figure 5.9 (a)** and the Aqua Nuchar PAC is shown in **Figure 5.8 (f)** and **Figure 5.9 (f)**. There is a clear trend for both types of carbon that were used showing that it takes longer for the atrazine to desorb from the carbon when there is SRNOM present in the water. This was expected because the SRNOM blocks the pores on the PAC particles and keeps the p-DCB from displacing the pre-adsorbed atrazine.

It was also hypothesized that since S-PAC has more external surface area than the PAC, the SRNOM would not block as many pores on the S-PAC and therefore the desorption kinetics of atrazine with SRNOM in the water would be faster on the S-PAC. This is because of the greater specific surface area of the smaller particles of WC800 and Aqua Nuchar, and from the shorter internal diffusion path into these smaller particles. More atrazine is being displaced from the smaller carbon particles faster because it is not adsorbed as deeply into the particles as on the PAC and therefore it can be displaced easier. The internal diffusion length into the S-PAC particles is shorter and consequently the diffusion rate into and out of the particles will also be lower (Ando et al., 2010). Since S-PAC has more external surface area than PAC, there are a larger number of adsorption sites for NOM on the S-PAC than the PAC (Matsui et al., 2011, 2012). On S-PAC the external surface area is not bound inside a pore, so even if the NOM adsorbed it doesn't block other adsorption sites, whereas with internal surface area, NOM can sit at the entrance and prevent internal sites from being utilized. This pore-blockage effect can be seen below in **Figure 5.7** where some of the large dissolved organic molecules are blocking access to internal adsorption sites. There is also a fraction of smaller molecular weight SRNOM that is competing directly with the atrazine for adsorption sites on the carbon.

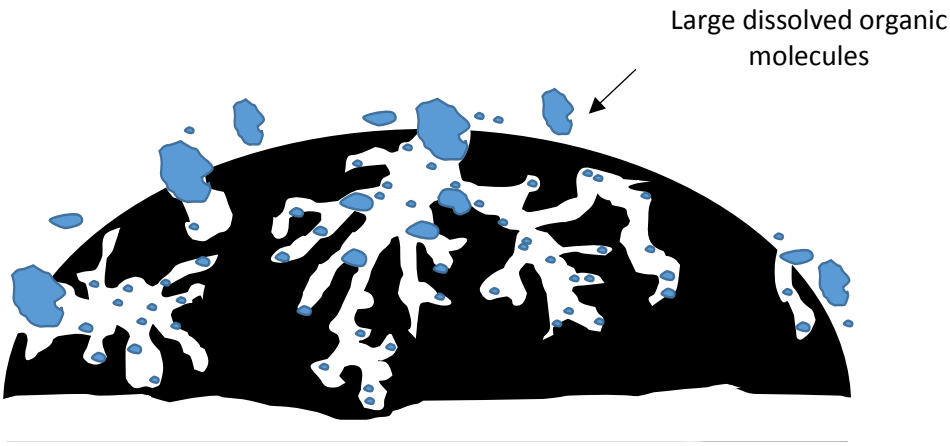

Figure 5.7 Large dissolved organic molecules creating pore-blockage on an activated carbon particle. Adapted from http://www.pacificwater.com.au/product/granular-activated-carbon-coconutshell/.

Based on **Figure 5.8** the S-PAC desorption kinetics with and without SRNOM are very similar whereas the PAC desorption kinetics with and without SRNOM are not as similar. As expected, the SRNOM did not slow down the desorption as much on the S-PAC as it did on the PAC. Amaral et al. found that the presence of SRNOM reduced the atrazine removal on PAC by around 35% and by 48% on 1 pass. On the 30 minute milling time the atrazine removal was only reduced by 13%, on the 1 hour it was only reduced by 4% and on the 6 hours by 36% (2016). This indicates that NOM competition is less intense for most of the S-PACs when compared to the PACs. The desorption results shown below in **Figure 5.8** and **Figure 5.9** are supported by these adsorption results because the desorption kinetics are also greater on the PAC than the S-PAC for both types of carbon in the presence of SRNOM. To et al. found that if most of the adsorption sites on activated carbon are occupied with a target compound, the buildup of pore-blocking NOM is actually desirable for hindering strongly competing contaminant uptake and micropollutant release (2008a).

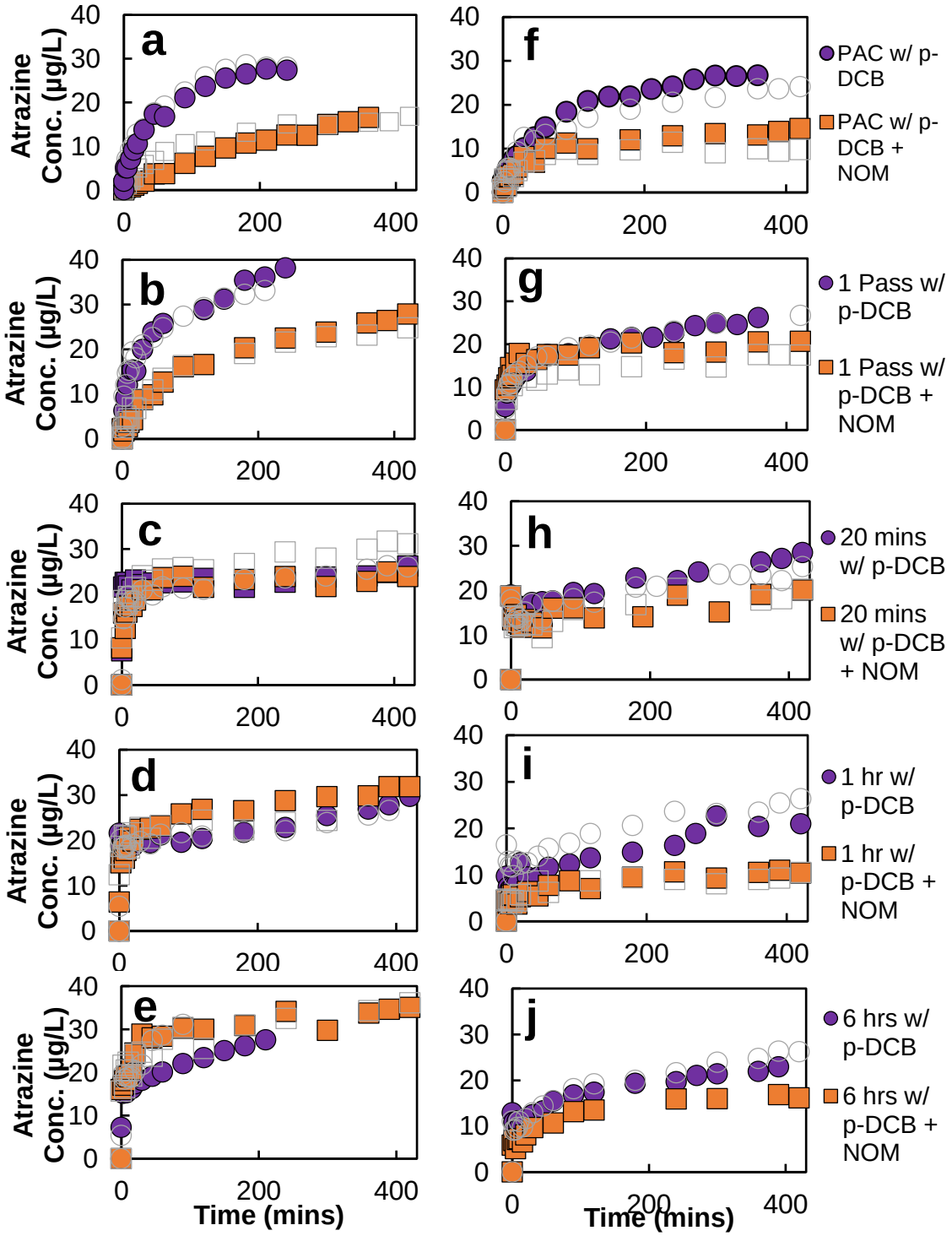

Figure 5.8 Desorption kinetics of atrazine on (a) WC800 PAC (b) WC800 1 Pass (c) WC800 30 minutes (d) WC800 1 hour (e) WC800 6 hours (f) Aqua Nuchar PAC (g) Aqua Nuchar 1 Pass (h) Aqua Nuchar 20 minutes (i) Aqua Nuchar 1 hour and (j) Aqua Nuchar 6 hours, all with and without SRNOM and with replicates shown in gray in the background. An easier way look at this figure is to note that the WC800 is in the left column and the Aqua Nuchar is in the right column with increased milling times in each row.

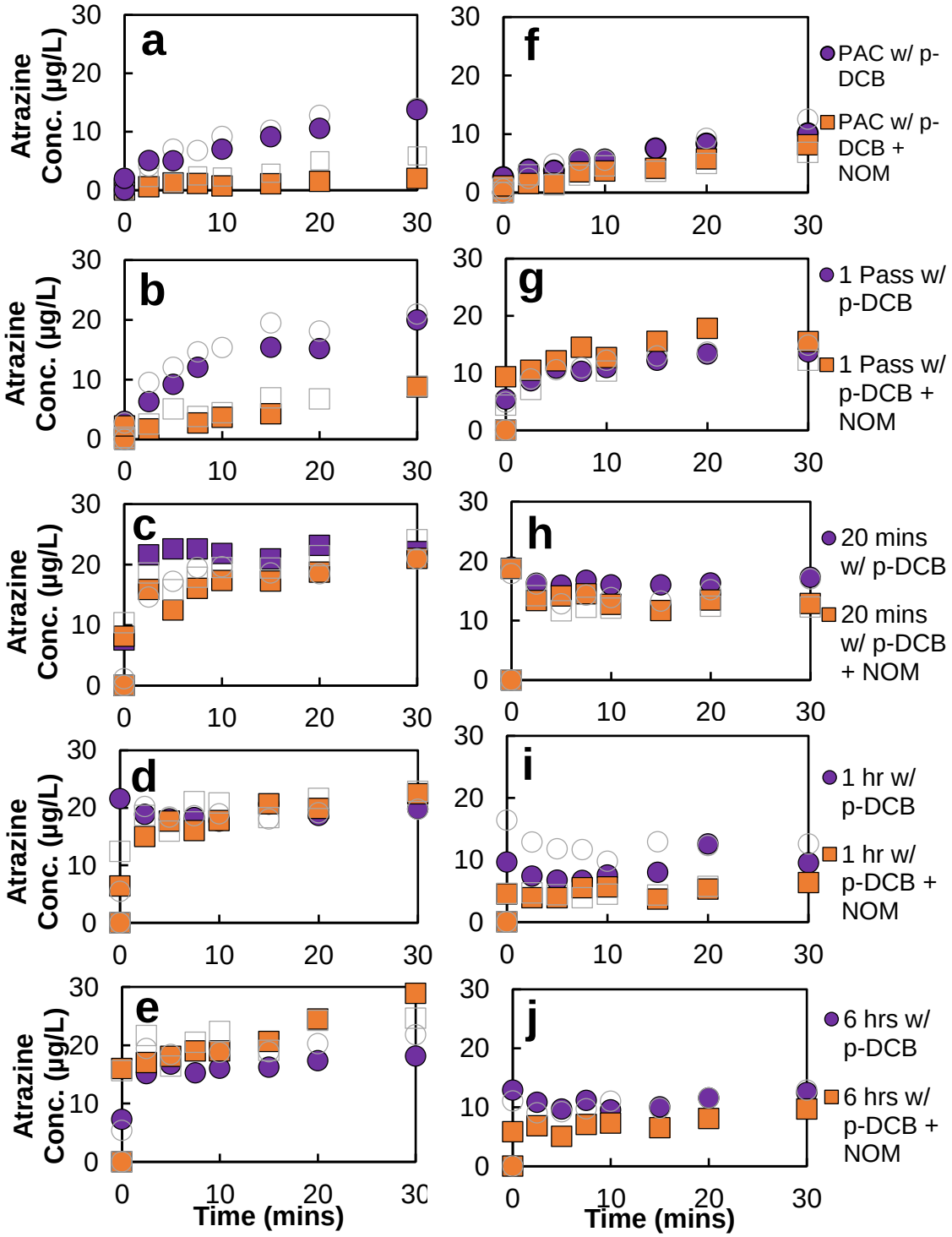

Figure 5.9 Desorption kinetics of atrazine on WC800 and Aqua Nuchar as shown in **Figure 5.8**, with different horizontal and vertical axes displayed to more clearly observe the differences in the desorption kinetics.

The desorption rates of the WC800 and Aqua Nuchar PAC and S-PACs with competition from pore blocking organic matter and strongly competing matter were also estimated by fitting a kinetic desorption equation through the data, which can be seen in **Equation 5.1**. The desorption rates, k, for each carbon type and milling time are shown in **Table 5.2**.

Table 5.2 Desorption rate for WC800 and Aqua Nuchar with competition from pore blocking organic matter and strongly competing matter, determined by fitting a kinetic desorption equation through the data. The goodness of fit (R-Square) value from the model is also reported.

Carbon	Desorption Rate, k (min^{-1})	R-square	Carbon	Desorption Rate, k (min^{-1})	R-square
WC800			**Aqua Nuchar**		
PAC	0.0094	0.99	PAC	0.0371	0.97
1 pass	0.0151	0.99	1 pass	0.3198	0.80
30 mins	0.5523	0.76	20 mins	1.1830	0.81
1 hr	0.3209	0.75	1 hr	0.1196	0.55
6 hrs	0.3073	0.46	6 hrs	0.1045	0.54

Activated carbons are relatively soft materials. Commercial coal and wood based carbons have a Mohs hardness between 2 and 3 on the Mohs hardness scale, which ranges from 1 to 10 (Patni et al., 2008). Dunn found that coconut and wood based PAC had higher adsorption capacity and kinetics than coal based PAC (2011). This supports the higher estimated desorption rates that were found Aqua Nuchar PAC when compared to WC800 PAC both with and without SRNOM.

The PAC particle sizes for the WC800 and the Aqua Nuchar were very similar, however the Aqua Nuchar had a higher resistance to milling and did not decrease in particle size as fast as the WC800. WC800 PAC has a measured specific surface area of 644 m^2/g and a measured specific

pore volume of 0.35 cm^3/g while Aqua Nuchar PAC has a measured specific surface area of 1676 m^2/g and a measured specific pore volume of 0.89 cm^3/g (Partlan et al., 2015). Amaral et al. found that the wood based carbon had the highest surface area as well as the largest change with milling time, but these changes did not correlate with atrazine removal. This supports the estimated desorption rates that were found above for Aqua Nuchar both with and without pore blocking organic matter, which did not correlate with milling time either. However, for WC800, the bituminous coal based carbon, atrazine removal increased with milling until the 6 hour milling time. It is likely that Aqua Nuchar had thinner pore walls than other carbons, as indicated by the higher specific surface area, and thus had channels that were easily crushed during milling resulting in a decreased surface area with increased milling time, which the WC800 did not exhibit (Partlan et al., 2016).

5.3 Extended Time Experiments

It was originally expected that the atrazine concentration would start to reach equilibrium during the strongly competing matter desorption experiments after about 4 hours and that it would start to reach equilibrium after about 8 hours for the desorption experiments with pore blocking organic matter and strongly competing matter combined. After running a few sets of each type of experiment, it was found that the atrazine concentration did not equilibrate as fast as was initially expected. The main motivation of this work was to study the early desorption kinetics. However, a few sets of each experiment were run for up to three days each to see how long it took for the atrazine concentration to reach equilibrium. These experiments are shown in **Figure 5.10 (a)** and **Figure 5.10 (b)** below. As seen here, it took approximately two days for the atrazine concentration to equilibrate during desorption. When preloading the atrazine on the

carbon, equilibrium was only checked after 7 days of tumbling on a rotary tumbler and found to be equilibrated. It is important to know how long the atrazine desorption takes to reach equilibrium in order to model the data and find the atrazine desorption diffusion coefficients.

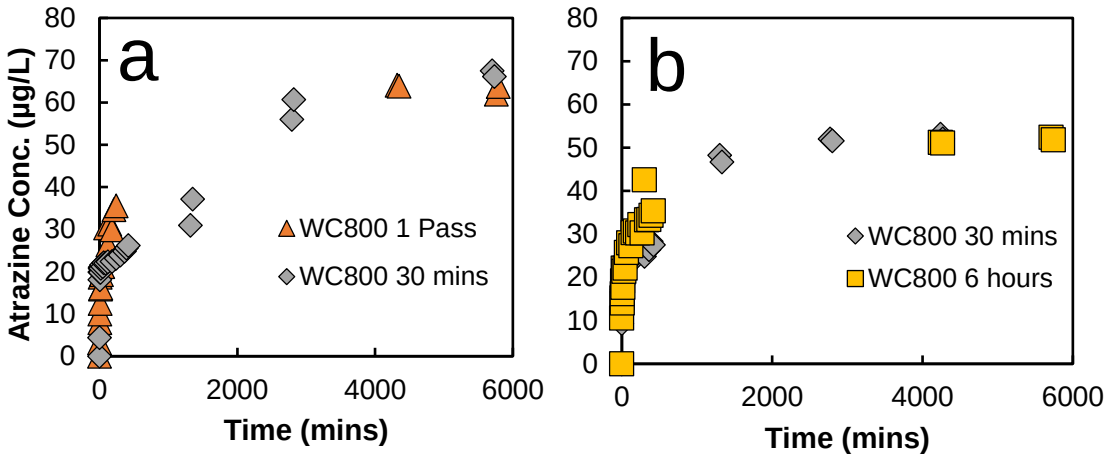

Figure 5.10 Extended time experiments for (a) strongly competing matter only and (b) pore blocking organic matter and strongly competing matter.

5.4 HSDM Modeling

The HSDM model was solved under pseudo-single-solute assumptions, in which p-DCB competition caused the carbons equilibrium adsorption capacity for atrazine to decrease, described as a reduction of atrazine's Freundlich isotherm adsorption capacity parameter, K. K_f and 1/n were used as inputs to solve for the best-fitting diffusion coefficient (D_S) for the WC8000 carbon. The best fitting diffusion coefficient was found using a MATLAB model developed by To (To, 2008) and can be seen in **Appendix 7.4** along with the other functions required to run the model. The experimental desorption kinetics are input into the DsSearch program, along with experimental and equilibrium conditions. The program searches for the best fitting diffusion coefficient using the HSDM and outputs the concentration data for the best

fitting kinetic curve. The Freundlich adsorption isotherms for WC800 were chosen because of how well they fit the model to the data. An example of the input excel file for WC800 PAC can be seen below in **Figure 5.11**.

	A	B	C	D	E	F	G	H	I	J
1		Experimental Data								
2		Time (min)	C (ug/L)		Parameter Type	Values	Variable	Units	Description	
3		0	4.8985			WC800 PAC	ID	-	name to identify this data set	
4		0.1	6.9241			4.89845	Co	µg/L	initial liquid concentration of trace compound	
5		2.5	9.4877		Mass	19.02031	qo	µg/mg	initial solid-phase concentration of trace compound	
6		5	10.912			5	Cc	mg/L	carbon concentration	
7		7.5	12.716		Particle	6.15	R	µm	particle radius	
8		10	13.001			70	nr	-	number or radial increments	
9		15	14.583		Time	250	tf	min	end time	
10		20	16.577			5	dt	min	incremental time step	
11		30	18.761		Equilibrium	3.44	Kf	µg/mg * (L/µg)1/n	Freundlich equilibrium K parameter for trace compound	
12		45	22.338			0.347	1/n	-	Freundlich equilibrium 1/n parameter for trace compound	
13		60	22.812			1.20E-10	Ds, guess 1			
14		90	26.61			1.21E-10	Ds, guess 2			
15		120	29.649		Kinetic	1.22E-10	Ds, guess 3	cm2/min	Diffusivity	
16		150	31.453			1.23E-10	Ds, guess 4			
17		180	32.434				Ds, guess 5			
18		210	32.726		Plot results?	yes				
19		240	32.6		Write data to file?	yes				
20										
21										

Figure 5.11 Example of the WC800 PAC excel input file for the DsSearch function in MATLAB that finds the best fitting diffusion coefficient.

The best fitting diffusion coefficient for WC800 PAC was found to be 1.2 x 10^{-10}, which can be seen below in **Figure 5.12**. It can also be seen that the model fit the data relatively well, however, the input parameters K_f and 1/n were not found experimentally. Freundlich adsorption isotherms for WC800 PAC would need to be completed to find the actual input parameters required for modeling using the HSDM.

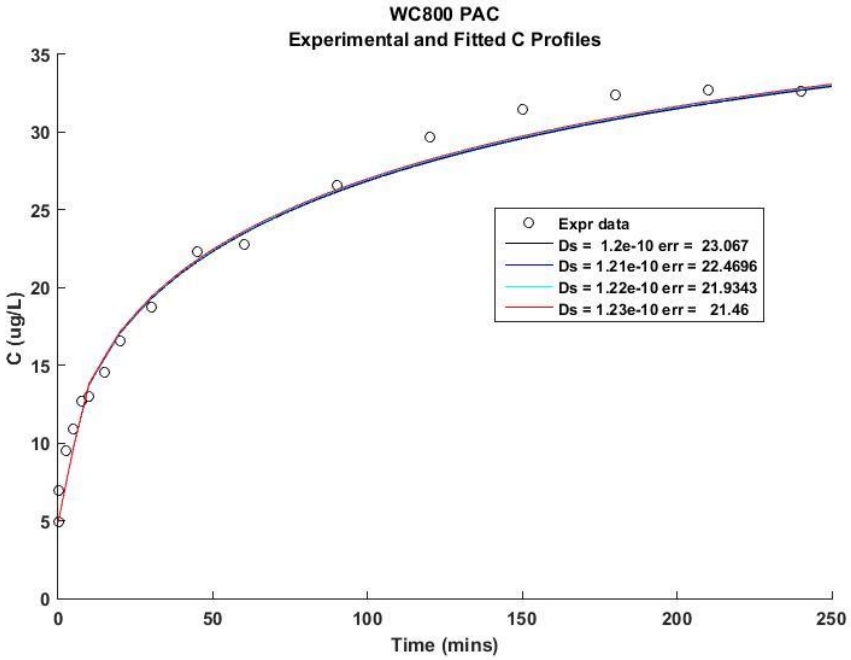

Figure 5.12 DsSearch output from MATLAB which shows the best fitting diffusion coefficient plot for WC800 PAC.

6 CONCLUSIONS AND RECOMMENDATIONS

The conclusions obtained from each initial objective of the research are listed below as follows:

Objective 1: The desorption kinetics are faster for S-PAC than PAC for Aqua Nuchar and WC800, however after the 30 minute milling time it is harder to distinguish the trend in desorption kinetics and milling time, which is consistent with adsorption kinetics data. There also appears to be a peak milling time reached before the desorption rates begin to decrease. For the WC800 carbon, the desorption rate increases with milling time until the 6 hour milling time was reached and for the Aqua Nuchar carbon, the desorption rate increases with milling time until the 1 hour milling time was reached.

Objective 2: SRNOM causes more pore blockage on PAC than on S-PAC for WC800 and Aqua Nuchar due to the increased specific external surface area on the S-PAC particles, resulting in more adsorption sites for SRNOM. On S-PAC the external surface area is not bound inside a pore, so even if the NOM is adsorbed, it doesn't block other adsorption sites, whereas with internal surface area, NOM can sit at the entrance and prevent internal sites from being utilized. Because of this, there is less competition on the S-PAC from SRNOM than there is on the PAC, therefore the desorption kinetics on S-PAC are faster than on the PAC when SRNOM is present in the water. The desorption kinetics for both PAC and S-PAC are faster without SRNOM in the water because there no pore blockage to slow the desorption of atrazine from the carbon. This difference is easier to see on the PAC kinetics because there is less external surface area on the PAC and more pore blockage. Even though there are more external adsorption sites on the S-

PAC, it is still believed that there are some internal pores and NOM can have a small pore blockage effect.

Recommendations for Future Work:

Some future work that will be important in further understanding S-PAC characteristics include modeling all of the S-PAC data using the HSDM and finding the Freundlich adsorption isotherms in order use the HSDM more accurately. The Freundlich adsorption isotherms will help determine the constants, K_f and 1/n, which are the adsorption capacity parameters needed to solve for the best fitting diffusion coefficient.

Also, varying the p-DCB and SRNOM concentrations to determine if desorption kinetics are easier to see at different concentrations could help us further understand S-PAC characteristics. It was suspected that the initial desorption kinetics on S-PAC are happening too fast to see. Lowering the p-DCB concentration could make these desorption kinetics easier to measure because they would be happening at a slower rate.

Measuring the desorption kinetics on milling times in between 1 hour and 6 hours will also help better distinguish between trends in milling time and desorption kinetics. There is a large milling time difference between 1 hour and 6 hours. If it could be determined what the desorption kinetics were on different S-PACs between these two milling times, it could lead to a better understanding of the optimum milling time for S-PAC, since it has been suggested that S-PAC milled for too long has diminishing returns. Finally, measuring the non-displaced desorption kinetics on S-PAC will help improve the understanding of S-PAC characteristics. This could be done by preloading the carbon with atrazine in the same way, and then removing the

background solution and replacing it with DDI water to see the desorption kinetics as atrazine desorbs back into the solution to create an equilibrium.

7 APPENDICES

7.1 Repeatability of Experiments

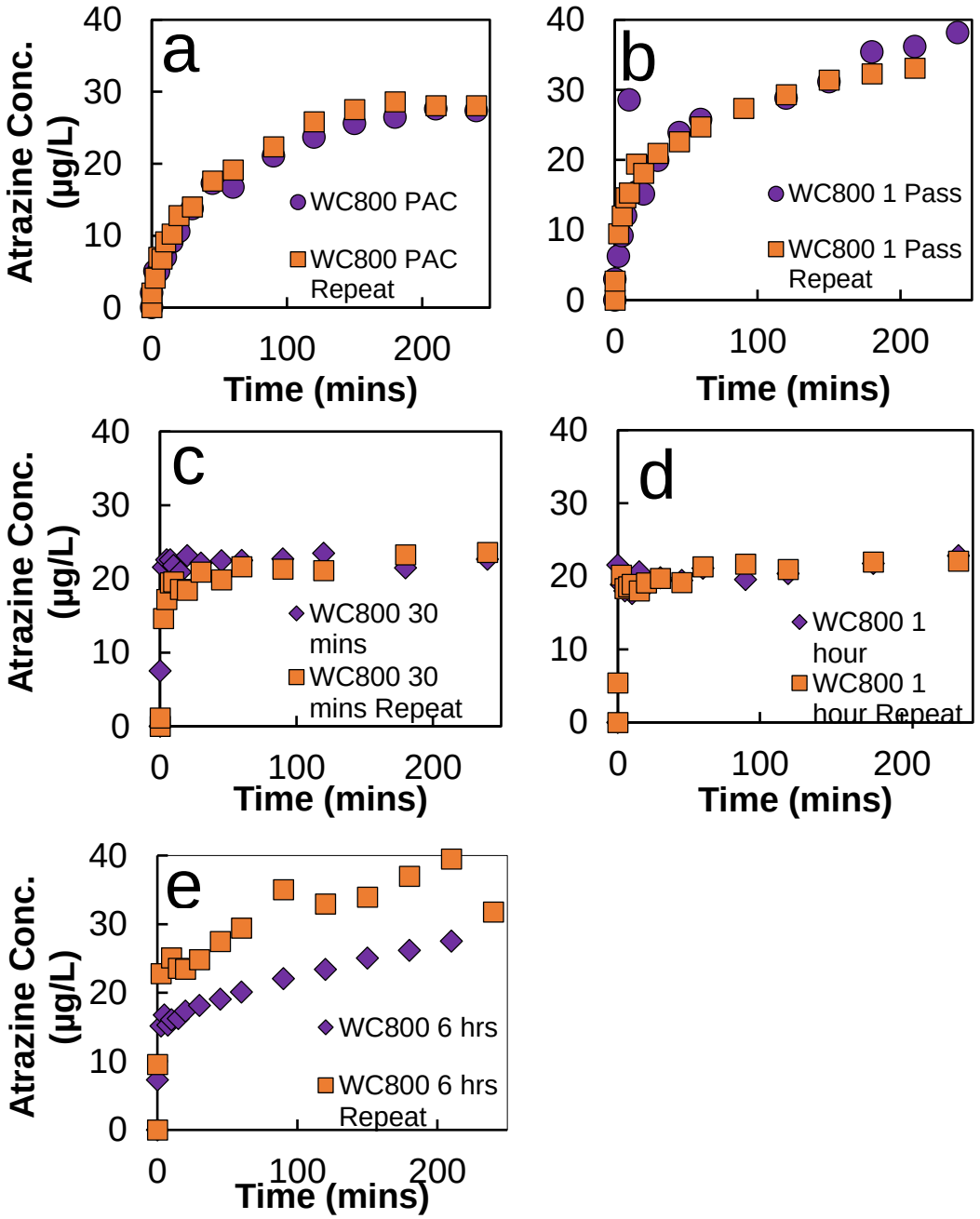

Figure 7.1 Repeat experiments using only strongly competing matter for WC800 (a) PAC, (b) 1 pass, (c) 30 minutes, (d) 1 hour, and (e) 6 hours.

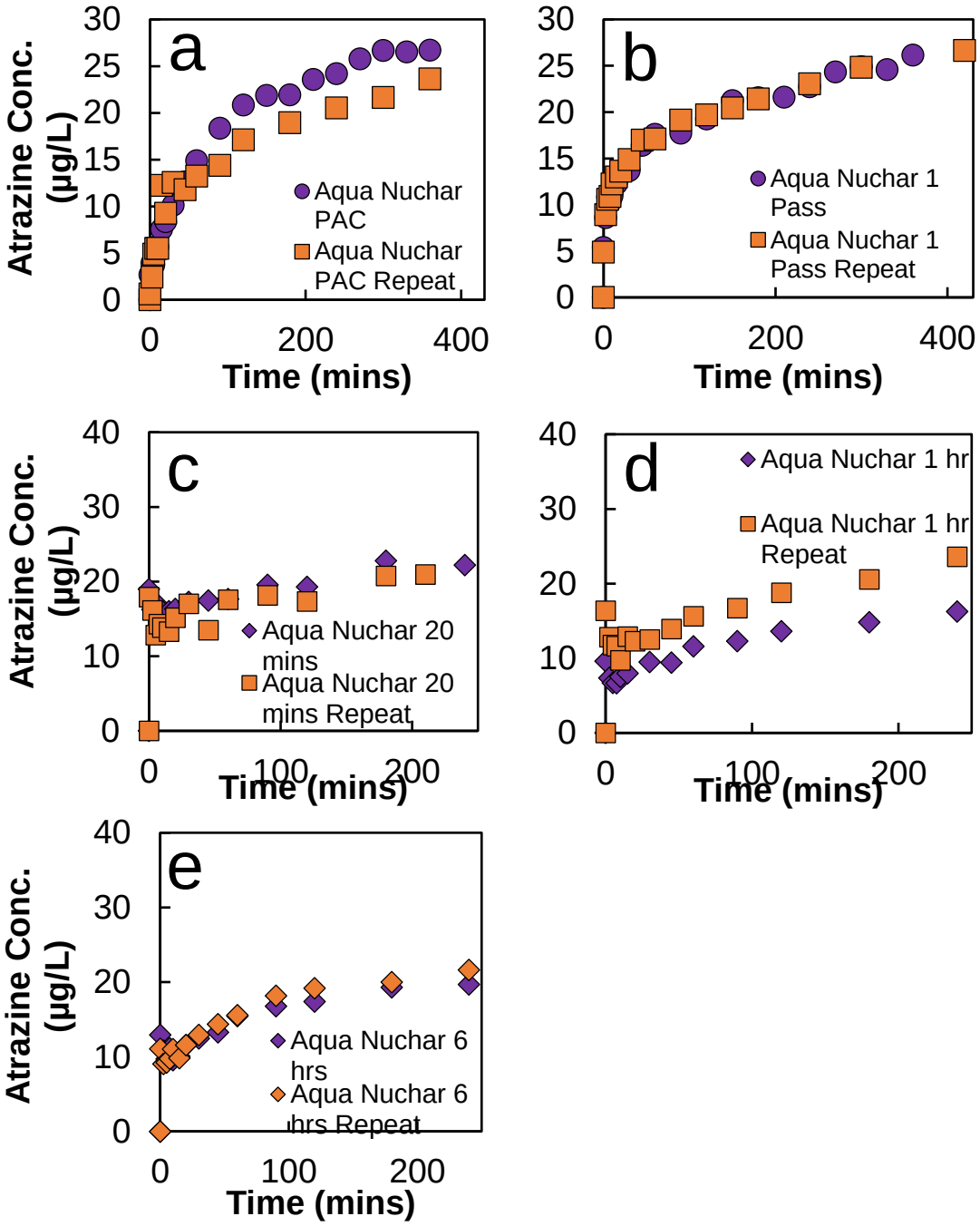

Figure 7.2 Repeat experiments using only strongly competing matter for Aqua Nuchar (a) PAC, (b) 1 pass, (c) 20 minutes, (d) 1 hour, and (e) 6 hours

One of the first things that was tested was the repeatability of the experiments. This was done by replicating all of the experiments that were completed to ensure that the kinetics of the two experiments were similar. Two examples of repeats for each type of carbon are shown below in **Figure 7.1** and **Figure 7.2**. Based on these figures, the experimental setup was assumed to be in proper working order. The data points from the first run and the repeat run are similar and show the same trend. This was completed for all other milling times and for the experiments involving pore blocking matter as well.

7.2 Preparation of Radiolabeled Atrazine Stock Solution

Calculation of Atrazine Volume

- The concentration of atrazine is 100 ppb (labeled: non-labeled=1:299)
- The concentration is not various in this procedure
- Assume the feed solution that is needed is 2000 mL
- The mass of atrazine is 100 ppb × 2000 mL= 0.2 mg/L × 1000mL × 1 L / 1000 mL=0.2 mg
- Labeled atrazine: 0.2 mg × 1/300 = 6.667 × 10^ (-4) mg
- The stock solution of labeled atrazine is 1.34 mg/L
- Non-labeled atrazine: 0.2 mg × 299/300 = 0.19933 mg
- The stock solution of non-labeled atrazine is 0.1 mg/mL
- The volume of labeled stock solution needed is 6.667 × 10^ (-4) mg / 1.34 mg/L = 0.4975 × 10^ (-3) L= 497.5 μL
- The volume of non-labeled stock solution needed is 0.19933 mg / 0.1 mg/mL = 1.9933 mL
- Add the stock solution in volumetric flask and then add DDI to scale mark

Preparation of the Calibration Curve

- Prepare atrazine at 0 ppb, 0.098 ppb, 0.195 ppb, 0.391 ppb, 0.781 ppb, 1.563 ppb, 3.125 ppb, 6.25 ppb, 12.5 ppb, 25 ppb, 50 ppb, and 100 ppb
- Take 5 mL stock solution of the volumetric flask and move it to a plastic vial (20mL)
- Mark this vial as 15 ppb
- Repeat the step above and mark it as 7.5 ppb
- Add 5 mL of DDI into 7.5 ppb vial to make the concentration 7.5 ppb
- Take 5 mL of the solution of 7.5 ppb vial into a new plastic vial and mark as 3.75 ppb.
- Dilute the solution in the vial using 5 mL of DDI and repeat the steps above to get the calibration curve
- 0 ppb concentration is added 5 mL of DDI
- Add scintillation cocktail into these vials

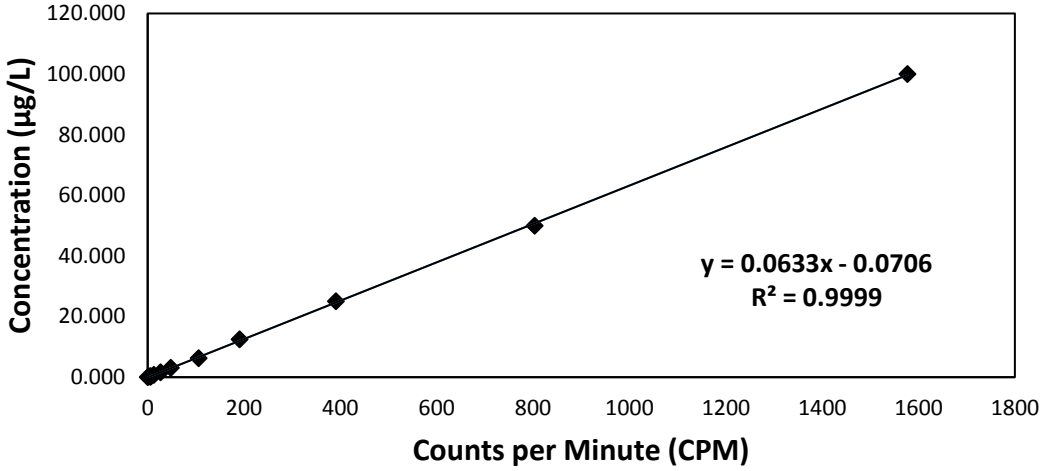

Figure 7.3 Calibration Curve of Radiolabeled Atrazine with Carbon-14.

7.3 MATLAB Curve Fitting Tool to Find Desorption Rate

The MATLAB curve fitting tool was used to determine the desorption rate of atrazine on the WC800 and Aqua Nuchar PAC and S-PACs. The exponential decay equation in increasing form was modified to fit the trend of the data. The equation used was:

$$C = C_o - C_o * e^{-k*time} \quad (7.1)$$

where k is the desorption rate of the atrazine that is being displaced from the activated carbon, C_o is the final concentration of atrazine that was desorbed from the carbon, and C is the concentration of atrazine at a specified time. The desorption rates of atrazine on WC800 and Aqua Nuchar, along with the R-square value for the model can be found in **Table 5.1** and **Table *5.2***. Example images of the inputs and outputs used with the MATLAB curve fitting tool for WC800 PAC with strongly competing matter only are shown below in **Figure 7.4** and **Figure 7.5**. Example images of Aqua Nuchar 20 minutes with pore blocking organic matter and strongly competing matter are shown below in **Figure 7.6** and **Figure 7.7**. Finally, example images of the inputs and outputs used for Aqua Nuchar 6 hours with pore blocking organic matter and strongly competing matter are shown below in **Figure 7.8** and **Figure 7.9**. These three carbons were chosen to show examples of a range of the different R-square values found for the curve fittings.

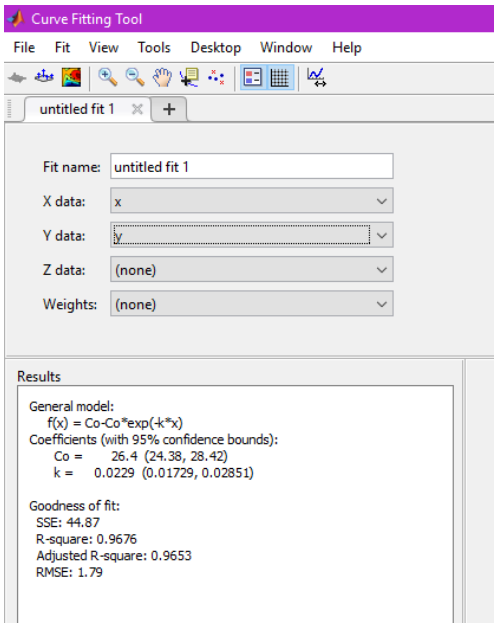

Figure 7.4 Input and output data for WC800 PAC with strongly competing matter only using the curve fitting tool in MATLAB.

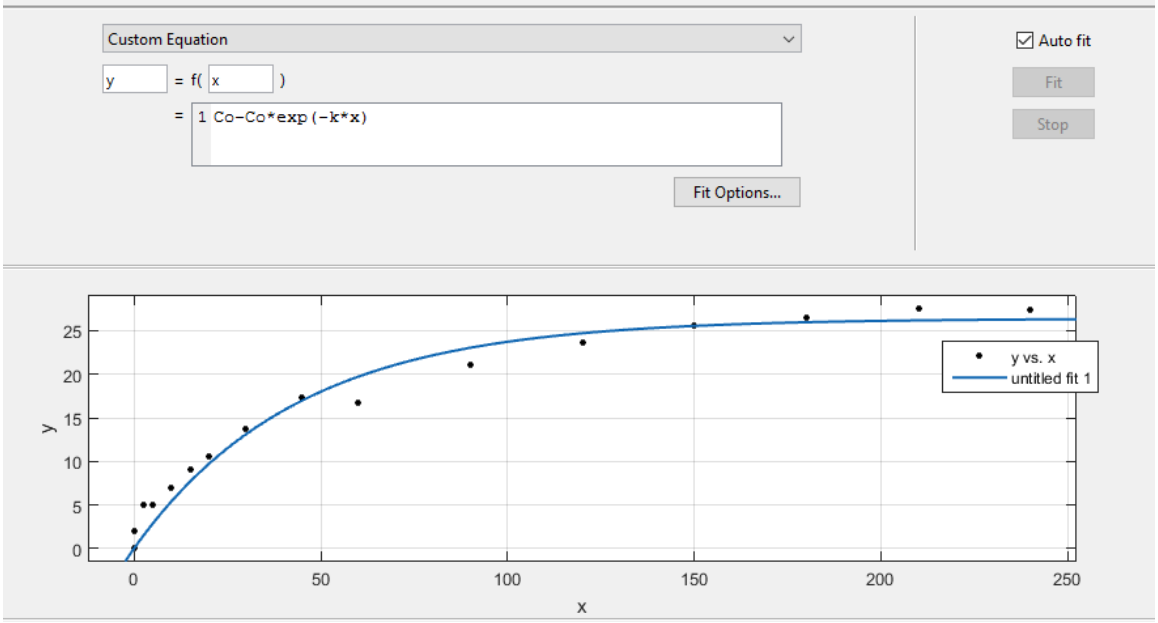

Figure 7.5 Input equation and output plot for WC800 PAC with strongly competing matter only using the curve fitting tool in MATLAB.

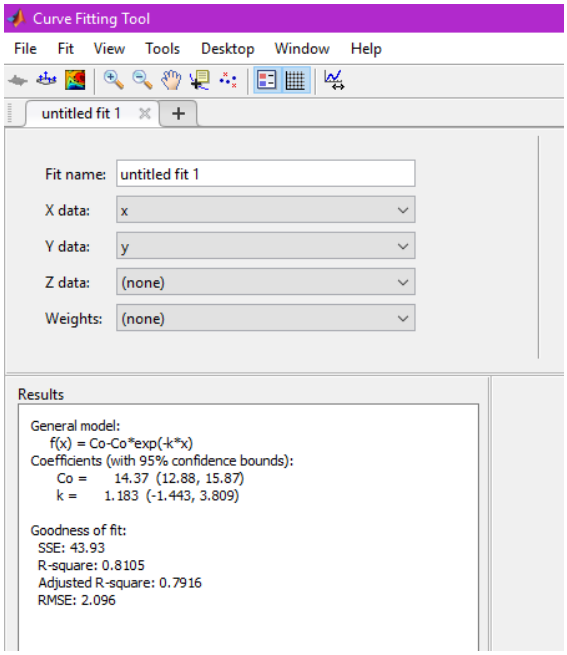

Figure 7.6 Input and output data for Aqua Nuchar 20 minutes with pore blocking organic matter and strongly competing matter using the curve fitting tool in MATLAB

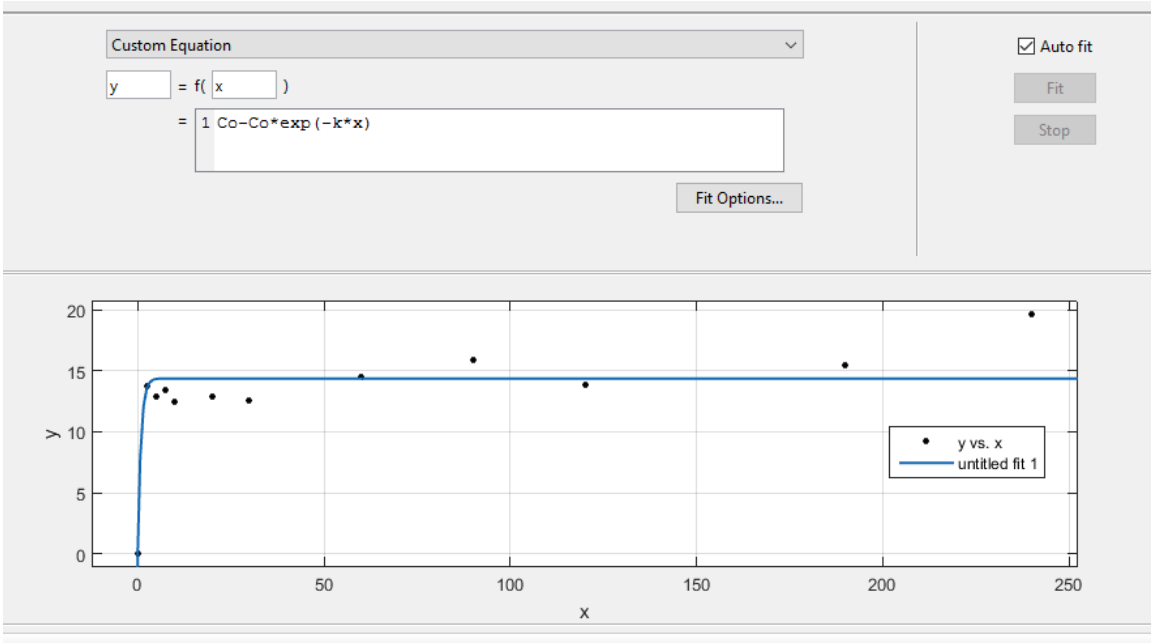

Figure 7.7 Input equation and output plot for Aqua Nuchar 20 minutes with pore blocking organic matter and strongly competing matter using the curve fitting tool in MATLAB.

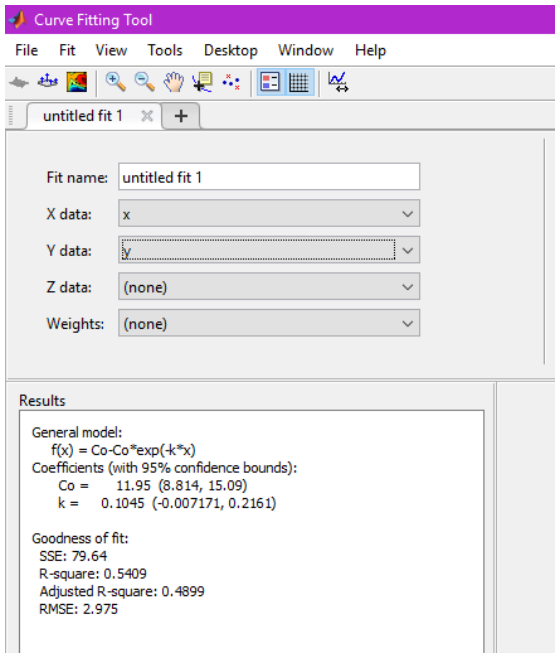

Figure 7.8 Input and output data for Aqua Nuchar 6 hours with pore blocking organic matter and strongly competing matter using the curve fitting tool in MATLAB

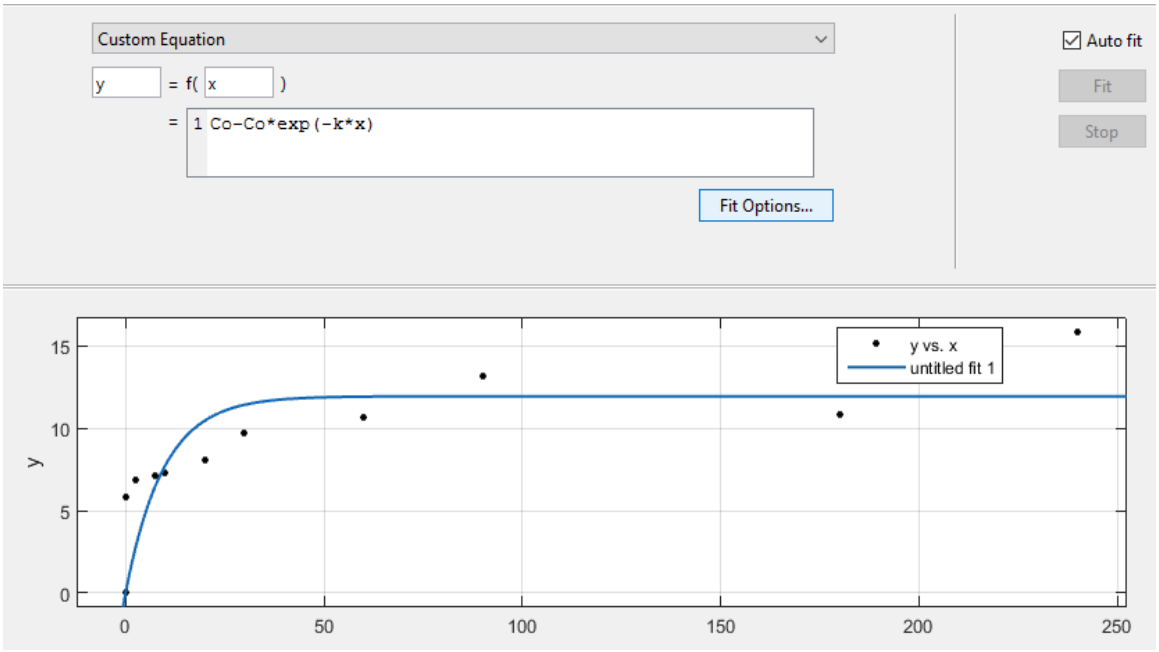

Figure 7.9 Input equation and output plot for Aqua Nuchar 6 hours with pore blocking organic matter and strongly competing matter using the curve fitting tool in MATLAB.

7.4 HSDM MATLAB Codes

The MATLAB codes that were used are provided for the following m-files:

1. HSDM.m – outpouts curve plot and data from singleHSDM.m
2. DsSearch.m – solves for the best fitting D_s given experimental kinetic data
3. singleHSDM.m – calculates solute concentration profiles given D_s
4. nextdt.m – executes the Thomas method for tridiagonal matrix
5. finddiff.m – finds the difference between experimental kinetic data and calculated concentrations from singleHSDM.m
6. calc_qavg.m – finds average adsorbed concentration across spherical particle

7.4.1 HSDM

File Name: HSDM.m

```
function HSDM
% Author: Priscilla To
% Description: HSDM for PAC batch adsorption system
% Uses finite difference method to solve for solid-phase concentration
%     of trace of trace compound (u=gr)
% Assumes
% -instantaneous equilibrium on surface between bulk liguid-PAC as
%   described by Freundlich
% -spherical symmetry
% -well mixed system, neglect film diffusion at boundary
% -constant diffusivity and density

clear

% read input file (HSDM_in.xls)
% nf = 1/n

[inputfile,text] = xlsread('HSDMin.xlsx', 'C2:C15') ;
id = text (1) ;
plot = char(text(end-2)) ;
writeC = char(text(end-1) ) ;
writeq = char(text(end));
dt = inputfile (7); % min
Ds = inputfile (10); % cm^2/min

% call function singleHSDM to solve for C and q numerically
[C_final, q, time, rad, m, n] = singleHSDM (Ds, inputfile);

Co = inputfile (1); % ug/L
C_over_Co = 0;
```

```
if Co ~= 0
    C_over_Co = C_final./Co;
end
if (isequal(plot,'yes') == 1)
    plotresults (id, C_final, C_over_Co, time, q, rad, n, dt) ;
end
if (isequal(writeC,'yes') == 1)
    writeCresults(id, time, C_final, C_over_Co);
end
if (isequal(writeq,'yes') == 1)
    writeqresults(id, time, rad, q, m, n) ;
end
if (isequal(plot,'yes')==1) || (isequal(writeC,'yes')==1) || ...
        (isequal(writeq,'yes')==1)
    writeinput(id, inputfile);
end

% subfunctions

function plotresults (id, C_final, C_over_Co, time, q, rad, n, dt)
% Plot results of C/Co (or C if Co = 0)
subplot(1,2,1);

if C_over_Co == 0
    plot (time, C_final,'.b');
    ylabel ( 'C (ug/L) ') ;
else
    plot (time, C_over_Co,'.b');
    ylabel ( 'C/Co (ug/L) ' ) ;
end
xlabel('Time (min)');
title([id, 'C profile']);
hold on
subplot(1,2,2);
hold on
N = round([2; n/4; n/2; n*3/4; n] ) ;
T = int2str((N-1)*dt);
t = [ ' t = ' ; ' t = ' ; ' t = ' ; ' t = ' ; ' t = ' ] ;
min = [' min';' min';' min';' min';' min'];
legendlabels = cat(2, t, T, min);
plot (rad, q(2:end,N(1)) , '.m');
plot (rad, q(2:end,N(2)) , '.r');
plot (rad, q(2:end,N(3)) , '.c');
plot (rad, q(2:end,N(4)) , '.b');
plot (rad, q(2:end,N(5)) , '.k');
xlabel('Radius (um)');
ylabel ( 'q (ug/mg)' ) ;
title([id, 'q profile']);
legend (legendlabels);
hold off
return;

function writeCresults(id, time, C_final, C_over_Co)
```

```
% write C data to excel file with function write_xls
% writes results to excel file with name "id"

filename=char(id);
Clabel = {'Time(min)', 'C (ug/L)', 'C/Co'};
xlswrite(filename, Clabel, 'Sheet1','A1');
xlswrite(filename, time, 'Sheet1', 'A2');
xlswrite(filename, C_final', 'Sheet1', 'B2');
if C_over_Co ~= 0
    xlswrite(filename, C_over_Co', 'Sheet1','C2')
end
return

function writeqresults(id, time, rad, q, m, n )

% write q data to excel file with function write_xls
% writes results to excel file with name "id"
% Excel number of columns limited to 256

filename=char(id);
if n < 255
    qsmall = q;
    tsmall = time';
else
    qsmall = [ ] ;
    tsmall = [ ] ;
    for i = 1:ceil(n/255):n
        qsmall = [qsmall, q(:,i)];
        tsmall = [tsmall, time(i)];
    end
end
Qlabel = {'Time(min)'; 'Radius(um)='};
xlswrite(filename, Qlabel, 'Sheet3');
xlswrite(filename, rad, 'Sheet3','A3');
xlswrite(filename, tsmall, 'Sheet3', 'B1');
xlswrite(filename, qsmall(2:m,:), 'Sheet3','B3');
return;

function writeinput(id, inputfile)

% write input parameters to file

filename=char(id);
Labels = {'File ID'; 'Co (ug/L)'; 'qo (ug/mg)'; 'Cc (mg/L)';...
    'R (um)'; 'nr (-)'; 'tf (min)'; 'dt (min)'; ...
    'K (ug/mg*L/mg/vl/n) ' ; '1/n (-)'; 'Ds (cm^2/min) ' } ;
xlswrite(filename, Labels, 'Sheet2', 'A1');
xlswrite(filename, id, 'Sheet2', 'B1');
xlswrite(filename, inputfile(1:10), 'Sheet2', 'B2');
return;
```

7.4.2 D_sSearch

File Name: DsSearch.m

```
function DsSearch

% Author: Priscilla To
% Description: Fit Ds to experimental data using KSDM for batch
%   adsorption system. Requires initial guess for Ds.
%   If error is large, guess a new Ds.
% Uses finite difference method to solve for solid-phase concentration
%   of trace of trace compound (u=qr)
% Assumes
% -instantaneous equilibrium on surface between bulk liquid-PAC as
%   described by Freundlich
% -spherical symmetry
% -well mixed system, neglect film diffusion at boundary
% -constant diffusivity and density

clear

% read experimental data (input.xls)
% column 1 of data = Time (min)
% column 2 of data = Cone (ug/L)

[data] = xlsread('input.xlsx','A:B');

% read input parameters
% nf = 1/n

[inputfile,text] = xlsread('input.xlsx','F3:F19');
id = text(1);
plot = char(text(end-1));
write = char(text(end));
Dsguess = inputfile(10:end); % initial guesses for Ds

% fits input data to Ds, using least squares error

options = optimset ('Display','iter'); % set to display iterations

trackDs = [ ] ;
a = size (Dsguess);
for i = 1:1:a(1)
    [Ds,resnorm,residual,exitflag] = lsqnonlin
(@finddiff,Dsguess(i),0,...
        1e-8,options,data,inputfile);
    trackDs = [trackDs; Dsguess(i), Ds, resnorm, exitflag];
end
format short e
disp( ' ' ) ;
```

```
disp(' Guess Ds Search Ds Resnorm Exitflag');
disp(trackDs);

if ((isequal(write,'yes') == 1) | (isequal(plot,'yes') == 1))
    [trackC_final, trackq, time] = runHSDM (a, trackDs, inputfile);
    if (isequal(plot,'yes') == 1)
        plotresults (data, a, time, id, trackC_final, trackDs);
    end
    if (isequal(write,'yes') == 1)
        writeresults (id, time, inputfile, trackDs, trackC_final,
data);
    end
end


function diffarray = finddiff (Ds,data,inputfile);

% 1) Calc C and q profile by HSDM given Dsguess
% 2) Compare differences from data points to calcuated profiles.
%   If data does not match numerical
% 3) Returns an array of differences

[C_final, q , time, rad, m, n] = singleHSDM (Ds, inputfile);
diff = [];
C = [];
i = 1;
for i = 1:1:length(data)
    index = find(time > data(i,1))
    a = index (1);
    frac = (data(i,1) - time (a-1))/(time(a)-time(a-1));
    C = [C; frac * (C_final(a)-C_final(a-1)) + C_final(a-1)]
end
diffarray = data(:,2) - C;
return


function [trackC_final, trackq, time] = runHSDM (a, trackDs, inputfile)

% Runs HSDM model for fitted Ds

trackC_final = [];
trackq = [];
for i = 1:1:a(1)
    [C_final, q, time, rad, m, n] = singleHSDM
(trackDs(i,2),inputfile);
    trackC_final(:,i) = C_final';
    trackq = [trackq, q];
end
return
```

```
function plotresults (data, a, time, id, trackC_final, trackDs)

% Plots data and curve from search results

figure;hold on
plot (data(:,1),data( : ,2), 'ok');
for i = 1:1:a(1)
    if i==1          plot (time, trackC_final(:,1), '-k');
    elseif i==2      plot (time, trackC_final(:,2), '-b');
    elseif i==3      plot (time, trackC_final(:,3), '-c');
    elseif i==4      plot (time, trackC_final(:,4), '-r');
    else             plot (time, trackC_final(:,5), '-m');
    end
end

xlabel('Time (min)');
ylabel('C (ug/L) ') ;
title([id, 'Experimental and Fitted C Profiles']);
D = [ ] ;
E = [];
for i=1:1:a(1)
    D = [D; 'Ds = ' ];
    E = [E; ' err = ']
end
DD = num2str(trackDs(:,2));
EE = num2str(trackDs(:,3));
legendlabels = cellstr(cat(2, D, DD, E, EE));
legendlabels = cat(1, 'Expr data', legendlabels);
legend(legendlabels);
hold off
return


function writeresults (id, time, inputfile, trackDs,C_final, data);

% Subfunction writes results to excel file with name

filename=char(id);
T = {'Time (min)','C (ug/L)'};
D = {'Guess Ds(cmA2/min)'; 'Search Ds (cm^2/min)'; 'Error';
    'Exitflag' } ;
xlswrite(filename,D, 'Sheetl', 'A1');
xlswrite(filename,T, 'Sheetl', 'A5');
xlswrite(filename,time, 'Sheetl', 'A6');
xlswrite(filename,trackDs', 'Sheet1', 'B1');
xlswrite(filename,C_final, 'Sheet1', 'B6');

Labels = {'File ID', 'Co (ug/L)', 'qo (ug/mg)', 'Cc (mg/L)', 'R
(um)',...
    'nr (-)', 'tf (min)', 'dt (min)', 'K (ug/mg*L/mg^1/n)', '1/n (-)'};
xlswrite(filename, Labels', 'Sheet2', 'A1');
xlswrite(filename, id, 'Sheet2', 'B1');
```

```
xlswrite(filename, inputfile(1:9), 'Sheet2', 'B2');
E = {'Experimental Data'};
xlswrite(filename, E, 'Sheet2', 'D1');
xlswrite(filename, T, 'Sheet2', 'D2');
xlswrite(filename, data, 'Sheet2', 'D3');
return
```

7.4.3 SingleHSDM

```
File Name: singleHSDM.m
% Author: Priscilla To

function [C_final, q, time, rad, m, n] = singleHSDM (Ds, inputfile);

% Returns C_final and q profiles given input of Ds

Co = inputfile(1);        %ug/L
qo = inputfile(2);        %ug/mg
Cc = inputfile(3);        %mg/L
R = inputfile(4) * 1e-4;   %convert from um to cm
nr = inputfile(5);        %number of radial increments
tf = inputfile(6);        %min
dt = inputfile(7);        %min
Kf = inputfile(8);
nf = inputfile(9);

% define step size dr and dt

dr = R/nr;
m =(R/dr + 1) ;
n = tf/dt + 1;

% mass balances for total mass of trace compound in batch system

C_final(1) = Co;
Ctot = C_final(1) + qo * Cc;


% set up u(t=0) matrix for column vector (t=0 aka n=1)
% all u = qo*r

trackn = 1 ; % first time step, t=0
u = [];
for i = 1:1:m
    r = (i-1) * dr;
    u(i,trackn) = qo*r;
end
intm = int16(m);
qavg = calc_qavg(u(:,1),dr,R,m);
trackqavg(1) = qavg;
```

```
% Steps to solving at a single time step (repeat for each new time
      step):
% 1) Make initial guess for C(t=trackn)
% 2) Use guess to calculate uguess(r=R)= R * Kf * CAl/n
% 3) Use Crank-Nicholson/finite differences method to solve for
      u(r,trackn)
% 4) Use numerical integration to find q_avg = u/r
% 5) Use q_avg to calc C(t) = Ctot - q_avg*Cc
% 6) Compare C(t) to initial guess = error
% 7) Repeat 2 to 7, updating C(t) w/ new value until error w/in
tolerance

% Initial Guess

Cguess = 0;
uguess = R*Kf*Cguess^nf;

% set up tridiagonal constant matrix for simultaneous system of eqns to
% be solved by Thomas method

alpha = Ds * dt / (2* (dr)^2);
for i = 1:1:m-2
    a(i) = - alpha;
    b(i) = 1 + 2*alpha;
    c(i) = - alpha;
end
a(1) = 0;
c(intm-2)= 0;

% define d matrix

B = [];
for i = 1:1:m-3
    B(i,i) = 1 - 2 * alpha;
    B(i+1,i) = alpha;
    B(i,i+1) = alpha;
end
B(intm-2,intm-2) = 1 - 2 * alpha;
D = [ ] ;
for trackn = 2:1:n % solve for next time step
    Cguess = [];
    Ccalc = [];
    iter = 1;
    error = 1;
    while (abs(error(end)) > 1e-4)
        if iter == 1
            Cguess = 0;
            bound = Cguess;
        elseif iter ==2 % set next C(t) guess
            Cguess = [Cguess; Ccalc(end)];
        elseif (sign(error(end)) ~= sign(error(end-1)))
```

```
            bound = Cguess(end-1);
            Cguess = [Cguess; 0.5 * (Cguess(end) + bound)];
        else Cguess = [Cguess; 0.5 * (Cguess(end) + bound)];
        end
        uguess = R * Kf * double(Cguess(end))^nf;
        % ensure Cguess is double-precision
        D(intm-2) = alpha * (u(intm,trackn-1) + uguess);
        d = B * u(2:intm-1,trackn-1) + D'; % update d matrix
        utemp(1) = 0 ; % u(r=0) = 0
        utemp(2:intm-1) = nextdt(a,b,c,d); % solv by Thomas method
        utemp(intm) = uguess; % u(r=R) = u(m)
        qavg = calc_qavg(utemp,dr,R,m);

        Ccalc = [Ccalc; (Ctot - qavg * Cc)];
        error = [error; Cguess(end)-Ccalc(end)];
        iter = iter + 1;
    end
    C_final(trackn) = Cguess(end);
    u(:,trackn) = utemp';
    trackqavg(trackn) = qavg;
end

% create time array
% calculate q (not defined at r=0)

time = [];
for i = 0:dt:tf
    time = [time; i];
end
rad = [];
q= [ ] ;
for i = 2:1:m
    rad = [rad; (i-1)*dr*10000];
    q(i, :) = u(i,:)/((i-1)*dr);
end
```

7.4.4 Nextdt

```
File Name: nextdt.m
% Author: Priscilla To
% executes thomas method given input of tridiagonal elements

function [utemp] = nextdt (a,b,c,d);
utemp = [];
h = [ ] ;
P = [];
h(1) = [c(1)/b(1)];
p(1) = [d(1)/b(1)];
l = length(a);
```

```
for k = 2:1:l
    h(k) = c(k)/(b(k) - a(k)*h(k-1));
    p(k) = (d(k)-a(k)*p(k-1))/(b(k)-a(k)*h(k-1));
end
utemp(l) = p(l); % because h(l) = 0
for k = l-1:-1:1
    utemp(k) = p(k) - h(k) * utemp(k+1);
end
```

7.4.5 FindDiff

```
File Name: finddiff.m
% Author: Priscilla To

function diffarray = finddiff (Ds,data,inputfile);

% function to
% 1) Calc C and g profile by HSDM given Dsguess
% 2) Compare differences from data points to calcuated profiles.
%     If data does not match numerical steps, interpolate.
% 3) Returns an array of differences (not yet squared)

[C_final, q , time, rad, m] = singleHSDM (Ds, inputfile);

% find difference between data and calculated cone

diff = [];
C = [];
i = 1;
for i = 1:1:length(data)
      index = find(time > data(i,1));
      a = index (1);
      frac = (data(i,1) - time (a-1))/(time(a)-time(a-1));
      C = [C; frac * (C_final(a)-C_final(a-1)) + C_final(a-1)];
end
diffarray = data(:,2) - C;

return;
```

7.4.6 Calc_qavg

```
File Name: calc_qavg.m
% Author: Priscilla To
% calculate qavg = average g in spherical particle
% by numerical integration - trapezoidal rule
% requires input of a 1-dimensional array

function [qavg] = calc_qavg (u,dr,R,m);
```

```
sum=0;
for i = 1:1:m-1
    r1 = (i-1)*dr; % radius at i
    r2 = i * dr; % radius at i+1
    r1 = double(r1); % convert to double precision
    r2 = double(r2);
    u1 = u(i);
    u2 = u(i+1);
    sum = sum + (dr / 2 * (r1*u1+ r2*u2));
end;

qavg = 3/R^3 * sum;

return;
```

8 REFERENCES

Adham, S. S., Snoeyink, V. L., Clark, M., & Bersillon, J. L. (1991). Predicting and verifying organics removal by PAC in an ultrafiltration system. *American Water Works Association*, *83*(81).

Amaral, P., Partlan, E., Li, M., Lapolli, F., Mefford, T., Karanfil, T., & Ladner, D. A. (2016). Superfine powdered activated carbon (S-PAC) coatings on microfiltration membranes: Effects of milling time on contaminant removal and flux. *Water Research2*, *100*, 429–438.

Amy, G., & Cho, J. (1999). Interactions between natural organic matter (NOM) and membranes: Rejection and fouling. *Water Science and Technology*. http://doi.org/10.1016/S0273-1223(99)00649-6

Ando, N., Matsui, Y., Kurotobi, R., Nakano, Y., Matsushita, T., & Ohno, K. (2010). Comparison of natural organic matter adsorption capacities of super-powdered activated carbon and powdered activated Carbon. *Water Research*, *44*(14), 4127–4136. http://doi.org/10.1016/j.watres.2010.05.029

Ando, N., Matsui, Y., Matsushita, T., & Ohno, K. (2011). Direct observation of solid-phase adsorbate concentration profile in powdered activated carbon particle to elucidate mechanism of high adsorption capacity on super-powdered activated carbon. *Water Research*, *45*(2), 761–767. http://doi.org/10.1016/j.watres.2010.08.050

Bansal, R. C., & Goyal, M. (2010). *Activated carbon adsorption*.

Baup, S., Jaffre, C., Wolbert, D., & Laplanche, A. (2000). Adsorption of pesticides onto granular activated carbon: determination of surface diffusivities using simple batch experiments. *Adsorption*, *6*, 219–228.

Chi, F.-H., & Amy, G. L. (2004). Kinetic study on the sorption of dissolved natural organic matter onto different aquifer materials: the effects of hydrophobicity and functional groups. *Journal of Colloid and Interface Science*, *274*(2), 380–91. http://doi.org/10.1016/j.jcis.2003.12.049

Colombini, M. P., Fuoco, R., Giannarelli, S., Posp, L., & Trskova, R. (1998). Protonation and Degradation Reactions of s-Triazine Herbicides 1. *Risorgimento*, *245*, 239 –245.

Considine, R., Denoyel, R., Pendleton, P., Schumann, R., & Wong, S.-H. (2001). The influence of surface chemistry on activated carbon adsorption of 2-methylisoborneol from aqueous solution. *Colloids and Surfaces A: Physicochemical and Engineering Aspects*, *179*(2-3), 271–280. http://doi.org/10.1016/S0927-7757(00)00647-6

Corwin, C. J., & Summers, R. S. (2011). Adsorption and desorption of trace organic contaminants from granular activated carbon adsorbers after intermittent loading and throughout backwash cycles. *Water Research*, *45*(2), 417–426. http://doi.org/10.1016/j.watres.2010.08.039

Coughlin, R. W., Ezra, F. S., & Tan, R. N. (1968). Influence of chemisorbed oxygen in adsorption onto carbon from aqueous solution. *Journal of Colloid and Interface Science*, *28*(3), 386–396.

Crittenden, J. C., Luft, P., & Hand, D. W. (1985). Prediction of multicomponent adsorption equilibria in background mixtures of unknown composition. *Water Research*, *19*(12), 1537–1548. http://doi.org/10.1016/0043-1354(85)90399-9

Dastgheib, S. A., Karanfil, T., & Cheng, W. (2004). Tailoring activated carbons for enhanced removal of natural organic matter from natural waters. *Carbon*, *42*(3), 547–557. http://doi.org/10.1016/j.carbon.2003.12.062

Dunn, S. E. (2011). *Effect of powdered activated carbon base material and size on disinfection by-product precursors and trace organic pollutant removal*.

Dunn, S. E., & Knappe, D. R. U. (2013). *DBP Precursor and Micropollutant Removal by Powdered Activated Carbon (Web Report #4294)*. Denver, Colorado: Water Research Foundation.

Ebie, K., Li, F., Azuma, Y., Yuasa, A., & Hagishita, T. (2001). Pore distribution effect of activated carbon in adsorbing organic micropollutants from natural water. *Water Research*, *35*(1), 167–179. http://doi.org/10.1016/S0043-1354(00)00257-8

Ellerie, J. R., Apul, O. G., Karanfil, T., & Ladner, D. A. (2013). Comparing graphene, carbon nanotubes, and superfine powdered activated carbon as adsorptive coating materials for microfiltration membranes. *Journal of Hazardous Materials*, *261*, 91–8. http://doi.org/10.1016/j.jhazmat.2013.07.009

Fitzer, E., Kochling, K., Boehm, H., & Marsh, H. (1995). Recommended Terminology for the Description of Carbon as a Solid. *International Union of Pure and Applied Chemistry*, *67*(3), 473–506.

Franz, M., Arafat, H. A., & Pinto, N. G. (2000). Effect of chemical surface heterogeneity on the adsorption mechanism of dissolved aromatics on activated carbon. *Carbon*, *38*(13), 1807–1819.

Garcia, T., Murillo, R., Cazorla-Amoros, A., Mastral, A., & Linares-Solano, A. (2004). Role of activated carbon surface chemistry in the adsorption of phenanthrene. *Carbon*, *42*(8), 1683–1689.

Hansch, C., Leo, A., & Hoekman, D. (1995). Hydrophobic, electronic, and steric constants. In *ACS Professional Reference Book* (p. 17). Washington, DC: American Chemical Society.

Heijman, S. G. J., Hamad, J. Z., Kennedy, M. D., Schippers, J., & Amy, G. (2009). Submicron powdered activated carbon used as a pre-coat in ceramic micro-filtration. *Desalination and Water Treatment*, *9*(1-3), 86–91.

Hopman, R., Siegers, W., & Kruithof, J. (1995). Organic micropollutant removal by activated carbon fiber filtration. *Water Supply*, *13*, 3–4.

Karanfil, T., & Kilduff, J. (1999). Role of granular activated carbon surface chemistry on the adsorption of organic compounds. 1. Priority pollutants. *Environmental Science & Technology*, *33*(18), 3217–3224. http://doi.org/10.1021/es981016g

Karanfil, T., Kitis, M., Kilduff, J., & Wigton, A. (1999). Role of granular activated carbon surface chemistry on the adsorption of organic compounds. 2. Natural organic matter. *Environmental Science and Technology*, *33*(18), 3225–3233.

Kilduff, J. E., & Karanfil, T. (2002). Trichloroethylene adsorption by activated carbon preloaded with humic substances: effects of solution chemistry. *Water Research*, *36*(7), 1685–1698.

Kilduff, J. E., Karanfil, T., & Weber, W. J. (1998). TCE adsorption by GAC preloaded with humic substances. *American Water Works Association*, *90*(5), 76–89.

Kose, H. S. (2010). *The effects of physical factors on the adsorption of synthetic organic compounds by activated carbon and activated carbon fibers*. Clemson University.

Lee, S.-J., Choo, K.-H., & Lee, C.-H. (2000). Conjuctive use of Ultrafiltration with powdered activated carbon adsorption for removal of synthetic and natural organic matter. *Journal of Industrial and Engineering Chemistry*.

Lemley, A., Wagenet, L., & Kneen, B. (1995). Activated Carbon Treatment of Drinking Water. *Water Treatment Notes: Cornell Cooperative Extension, College of Human Ecology*, 1–6. Retrieved from http://waterquality.cce.cornell.edu/publications/CCEWQ-03-ActivatedCarbonWtrTrt.pdf

Li, L., Quinlivan, P. A., & Knappe, D. R. U. (2002). Effects of activated carbon surface chemistry and pore structure on the adsorption of organic contaminants from aqueous solution. *Carbon*, *40*, 2085–2100.

Li, Q., Mariñas, B. J., Snoeyink, V. L., & Campos, C. (2003). Three-component competitive adsorption model for flow-through PAC systems. 2. Model application to a PAC/membrane system. *Environmental Science & Technology*, *37*(13), 3005–3011. http://doi.org/10.1021/es020989k

Li, Q., Snoeyink, V. L., Campos, C., & Mariñas, B. J. (2002). Displacement effect of NOM on atrazine adsorption by PACs with different pore size distributions. *Environmental Science and Technology*, *36*(7), 1510–1515. http://doi.org/10.1021/es010870w

Li, Q., Snoeyink, V. L., Mariñas, B. J., & Campos, C. (2003a). Elucidating competitive adsorption mechanisms of atrazine and NOM using model compounds. *Water Research*, *37*, 773–784. http://doi.org/10.1016/S0043-1354(02)00390-1

Li, Q., Snoeyink, V. L., Mariñas, B. J., & Campos, C. (2003b). Pore blockage effect of NOM on atrazine adsorption kinetics of PAC: The roles of PAC pore size distribution and NOM molecular weight. *Water Research*, *37*, 4863–4872. http://doi.org/10.1016/j.watres.2003.08.018

Lowe, E., & Moore, D. (1962). Scintillation counter for simultaneous assay of H3 and C14 in gas-liquid chromatographic vapors *, *3*(3).

Luft, P. (1984). *Modeling of multicomponent adsorption onto granular activated carbon in mixtures of known and unknown composition*. Michigan Technological University, Houghton, MI.

Mangun, C. L., Benak, K. R., Economy, J., & Foster, K. L. (2001). Surface chemistry, pore sizes and adsorption properties of activated carbon fibers and precursors treated with ammonia. *Carbon*, *39*(12), 1809–1820.

Matsui, Y., Aizawa, T., Kanda, F., Nigorikawa, N., Mima, S., & Kawase, Y. (2007). Adsorptive removal of geosmin by ceramic membrane filtration with super-powdered activated carbon. *Journal of Water Supply: Research and Technology—AQUA*, *56*(6–7), 411. http://doi.org/10.2166/aqua.2007.017

Matsui, Y., Ando, N., Sasaki, H., Matsushita, T., & Ohno, K. (2009). Branched pore kinetic model analysis of geosmin adsorption on super-powdered activated carbon. *Water Research*, *43*(12), 3095–103. http://doi.org/10.1016/j.watres.2009.04.014

Matsui, Y., Ando, N., Yoshida, T., Kurotobi, R., Matsushita, T., & Ohno, K. (2011). Modeling high adsorption capacity and kinetics of organic macromolecules on super-powdered activated carbon. *Water Research*, *45*(4), 1720–1728. http://doi.org/10.1016/j.watres.2010.11.020

Matsui, Y., Hasegawa, H., Ohno, K., Matsushita, T., Mima, S., Kawase, Y., & Aizawa, T. (2009). Effects of super-powdered activated carbon pretreatment on coagulation and trans-membrane pressure buildup during microfiltration. *Water Research*, *43*(20), 5160–5170. http://doi.org/10.1016/j.watres.2009.08.021

Matsui, Y., Murai, K., Sasaki, H., Ohno, K., & Matsushita, T. (2008). Submicron-sized activated carbon particles for the rapid removal of chlorinous and earthy-musty compounds. *Journal of Water Supply: Research and Technology—AQUA*, *57*(8), 577. http://doi.org/10.2166/aqua.2008.070

Matsui, Y., Murase, R., Sanogawa, T., Aoki, N., Mima, S., Inoue, T., & Matsushita, T. (2004). Micro-ground powdered activated carbon for effective removal of natrual organic matter during water treatment. *Water Supply2*, *4*(4), 155–163.

Matsui, Y., Nakao, S., Sakamoto, A., Taniguchi, T., Pan, L., Matsushita, T., & Shirasaki, N. (2015). Adsorption capacities of activated carbons for geosmin and 2-methylisoborneol vary with activated carbon particle size: Effects of adsorbent and adsorbate characteristics. *Water Research*, *85*, 95–102. http://doi.org/10.1016/j.watres.2015.08.017

Matsui, Y., Nakao, S., Yoshida, T., Taniguchi, T., & Matsushita, T. (2013). Natural organic matter that penetrates or does not penetrate activated carbon and competes or does not compete with geosmin. *Separation and Purification Technology*, *113*, 75–82. http://doi.org/10.1016/j.seppur.2013.04.009

Matsui, Y., Sakamoto, A., Nakao, S., Taniguchi, T., Matsushita, T., Shirasaki, N., … Yurimoto, H. (2014). Isotope Microscopy Visualization of the Adsorption Profile of 2-Methylisoborneol and Geosmin in Powdered Activated Carbon. *Environmental Science and Technology*, *48*, 10897–10903.

Matsui, Y., Yoshida, T., Nakao, S., Knappe, D. R. U., & Matsushita, T. (2012). Characteristics of competitive adsorption between 2-methylisoborneol and natural organic matter on superfine and conventionally sized powdered activated carbons. *Water Research*, *46*(15), 4741–4749. http://doi.org/10.1016/j.watres.2012.06.002

Najm, I. N., Snoeyink, V. L., Richard, Y., & Lake, J. (1991). Effect of Initial Concentration of a SOC in Natural Water on Its Adsorption by Activated Carbon. *American Water Works Association*, *83*(8), 57–63.

Nam, S.-W., Choi, D.-J., Kim, S.-K., Her, N., & Zoh, K.-D. (2014). Adsorption characteristics of selected hydrophilic and hydrophobic micropollutants in water using activated carbon. *Journal of Hazardous Materials*, *270*(January), 144–52. http://doi.org/10.1016/j.jhazmat.2014.01.037

Newcombe, G., Morrison, J., & Hepplewhite, C. (2002). Simultaneous adsorption of MIB and NOM onto activated carbon. I. Characterisation of the system and NOM adsorption. *Carbon*, *40*, 2135–2146. http://doi.org/10.1016/S0008-6223(02)00097-0

Okada, K., Yamamoto, N., Kameshima, Y., & Yasumori, A. (2003). Adsorption properties of activated carbon from waste newspaper prepared by chemical and physical activation. *Journal of Colloid and Interface Science*, *262*(1), 194–199. http://doi.org/10.1016/S0021-9797(03)00108-5

Partlan, E., Davis, K., Ren, Y., Apul, O. G., Mefford, T., Karanfil, T., & Ladner, D. A. (2016). Effect of bead milling on chemical and physical characteristics of activated carbons pulverized to superfine sizes. *Water Research*, *89*, 161–170.

Pelekani, C., & Snoeyink, V. L. (1999). Competitive adsorption in natural water: Role of activated carbon pore size. *Water Research*, *33*(5), 1209–1219. http://doi.org/10.1016/S0043-1354(98)00329-7

Pelekani, C., & Snoeyink, V. L. (2000). Competitive adsorption between atrazine and methylene blue on activated carbon: the importance of pore size distribution. *Carbon*, *38*(10), 1423–1436. http://doi.org/10.1016/S0008-6223(99)00261-4

Pelekani, C., & Snoeyink, V. L. (2001). Kinetic and equilibrium study of competitive adsorption between atrazine and Congo red dye on activated carbon: The importance of pore size distribution. *Carbon*, *39*(1), 25–37. http://doi.org/10.1016/S0008-6223(00)00078-6

Qi, S., Adham, S. S., Snoeyink, V. L., & Lykins, B. W. (1994). Prediction and Verification of Atrazine Adsorption by PAC. *Journal of Environmental Engineering*, *120*(1), 202–218. http://doi.org/10.1061/(ASCE)0733-9372(1994)120:1(202)

Quinlivan, P. a., Li, L., & Knappe, D. R. U. (2005). Effects of activated carbon characteristics on the simultaneous adsorption of aqueous organic micropollutants and natural organic matter. *Water Research*, *39*(8), 1663–1673. http://doi.org/10.1016/j.watres.2005.01.029

Ran, Y., Xiao, H., Huang, W. L., Peng, P. A., Liu, D. H., Fu, J. M., & Sheng, G. Y. (2003). Kerogen in aquifer material and its strong sorption for nonionic organic pollutants. *Journal of Environmental Quality*, *32*(5), 1701–1709. Retrieved from <Go to ISI>://000185409500014

Ren, Y., Apul, O. G., Partlan, E., Ladner, D. A., & Karanfil, T. (2016). Adsorption kinetics of synthetic organic chemicals on superfine powdered activated carbon. *In Preparation*.

Sing, K. S. W., Everett, D. H., Haul, R. A. W., Moscou, L., Pierotti, L. A., Rouquerol, J., & Siemieniewska, T. (1985). International union of pure and applied chemistry physical chemistry division reporting physisorption data for gas/soils systems with special reference to the determination of surface area and porosity. *Pure Appl. Chemistry*, *57*, 603–619.

Snoeyink, V. L., & Chen, A. S. C. (1985). Removal of Organic Micropollutants by Coagulation and Adsorption. *Science of the Total Environment, The*, *47*, 155–167.

Snyder, S. a., Adham, S., Redding, A. M., Cannon, F. S., DeCarolis, J., Oppenheimer, J., … Yoon, Y. (2007). Role of membranes and activated carbon in the removal of endocrine disruptors and pharmaceuticals. *Desalination*, *202*(1-3), 156–181. http://doi.org/10.1016/j.desal.2005.12.052

Sontheimer, H., Crittenden, J. C., & Summers, R. S. (1988). *Activated Carbon for Water Treatment* (2nd ed.). Karlsruhe, Germany: DVGW-Forschungsstelle.

Summers, R. S., Knappe, D. R. U., & Snoeyink, V. L. (2010). *Adsorption of organic compounds by activated carbon*. (J. K. Edzwald, Ed.) (6th ed.). New York: McGraw-Hill and American Water Works Association.

Thacker, W. E., Snoeyink, V. L., & Crittenden, J. C. (1983). Desorption of compounds during operation of GAC adsorption systems. *American Water Works Association*, *75*(3), 144–149.

To, P. C. (2008). *Desorption of trace contaminants from activated carbon: Effect of strongly-competing and pore-blocking background organic matter on desorption kinetics*. University of Illinois at Urbana-Champaign.

To, P. C., Mariñas, B. J., Snoeyink, V. L., & Wun, J. N. (2008a). Effect of pore-blocking background compounds on the kinetics of trace organic contaminant desorption from activated carbon. *Environmental Science and Technology*, *42*(13), 4825–4830. http://doi.org/10.1021/es800058s

To, P. C., Mariñas, B. J., Snoeyink, V. L., & Wun, J. N. (2008b). Effect of strongly competing background compounds on the kinetics of trace organic contaminant desorption from activated carbon. *Environmental Science and Technology*, *42*(7), 2606–2611. http://doi.org/10.1021/es702609r

USEPA. (1986). *Safe Drinking Water Act*.

USEPA. (2015). Technical Factsheet on: Atrazine. Retrieved from https://safewater.zendesk.com/hc/en-us/sections/202366538

Wigmans, T. (1989). Industrial aspects of production and use of activated carbons. *Carbon*, *27*(1), 13–22. http://doi.org/10.1016/0008-6223(89)90152-8

Wu, F. C., Tseng, R. L., & Juang, R. S. (2001). Adsorption of dyes and phenols from water on the activated carbons prepared from corncob wastes. *Environmental Technology*, *22*(2), 205–13. http://doi.org/10.1080/09593332208618296

Yalkowsky, S., & He, Y. (2003). 1,4-dichlorobenzene and 1,3-dichlorobenzene. In *Handbook of aqueous solubility data* (pp. 207–208). Boca Raton, FL: CRC Press.